Tectonophysics 750 (2019) 177–202

Contents lists available at ScienceDirect

Tectonophysics

journal homepage: www.elsevier.com/locate/tecto

Cumulative deformation and original geometry of the Bushveld Complex

I.J. Basson[a,b]

[a] Tect Geological Consulting, Unit 3, Metrohm House, 20 Gardner Williams Avenue, 7130, South Africa
[b] Department of Earth Sciences, University of Stellenbosch, Private Bag X1, Matieland, 7602, South Africa

ARTICLE INFO

Keywords:
Bushveld Complex
Cumulative deformation
Structural history

ABSTRACT

A structural review and re-interpretation of the Bushveld Complex, based on 254 georeferenced maps from research, technical reports and geophysical surveys, suggests that its current geometry differs markedly from its original geometry. Broadly N–S flattening, left-lateral transpressional shearing along an interconnected fault network, steepening of cumulate layering and 10 km of uplift, to the north of the northern margin of the complex's main chamber, were accompanied by an eastward-verging escape structure (Burgersfort Bulge) and syn-cooling gap areas on its Western Limb. Southward-verging deformation was transmitted from the Villa Nora Fragment, via thrusting in the Rooiberg area, generating 50–70 km of southward displacement, uplift and erosional loss of the Northern Limb's western portion. A string of anomalous occurrences of Bushveld Complex units and dense areas outlined by unconstrained gravity isoshells suggest a further 170 km southward displacement through the center of the main chamber. The Southern Limb underwent predominantly right-lateral, ductile offset from the Western Limb along the Crocodile River and Rustenburg Faults, expressed by an in-line series of NNW-trending magnetic highs to the south of their mapped terminations. Left-lateral shearing and progressive splaying of a NNE-trending dyke swarm, to the west of an inflection point, provides strain markers for this offset and 35° anticlockwise rotation of the Burgersfort Bulge and central parts of the main chamber. Although recent work suggests that the complex cooled within 1 Myr, late-intrusion/syn-cooling, SSE-wards movement of its deeper, ductile, central parts, within at least 5–10 Myr after its initial intrusion, the Transvaalide Fold-and Thrust event and the expulsion of fluids to form the high-Ti igneous suite (HITIS) and related bodies, appear to have closely post-dated the complex's intrusion. Removal of the effects of cumulative strain produces a more equant complex, shortly after its intrusion, occupying an orthogonal network of normal faults and perpendicular, strike-slip, transverse faults.

1. Introduction

The Bushveld Complex has been the subject of an extensive research effort over the last 100 years. The main body of this large, layered igneous complex intruded, possibly due to intracratonic rifting (Eriksson et al., 1991; Eriksson and Reczko, 1995), into the volcano-sedimentary Pretoria Group of the late Archaean to early Proterozoic Transvaal Supergroup (Lenhardt and Eriksson, 2012; Fig. 1), with the complex's Northern Limb in contact with Archaean granite-gneiss basement. It outcrops over an area of > 65,000 km^2 (Cawthorn et al., 2006), has a total thickness of approximately 12,000 m (Eriksson et al., 2001) and is consequently the largest known body of its type. The complex essentially comprises a thick mafic component, the Rustenburg Layered Suite (RLS), a granitic component comprising the Lebowa Granite Suite (LGS) and the Rashoop Granophyre Suite (RGS). It is generally accepted that the complex intruded as a series of flat, sill-like sheets or fingers (Kruger, 2005; Clarke et al., 2009) between the overlying Rooiberg Group volcanics, dated at 2061 ± 2 Ma (Cawthorn and Walraven, 1998; Walraven, 1997) and the underlying Pretoria Group, consisting of a sequence of shales, secondary clastics and subordinate volcanics, and minor banded ironstones. It is only in the Northern Limb that there is a marked transgression across the Transvaal Supergroup (inset, Fig. 1). The Rooiberg Group volcanics, the extrusive component of the complex, are up to 6 km thick and represent one of the largest known provinces of silicic volcanic rocks, comprising a volume comparable to that of the RLS itself.

The complex's mafic component, the RLS, may be subdivided into five zones, from its base upwards, according to compositional changes (Cawthorn et al., 2006) and marker units. The Marginal Zone, with a maximum thickness of 250 m, comprises gabbronorite, norite and various metasediments (Vermaak and Hendricks, 1976; Kruger, 2005) and is considered to be a chill margin containing metasedimentary xenoliths at the complex's base (Kruger, 2005). The overlying Lower Zone shows significant thickness variations, probably due to sub-outcropping

E-mail address: ianbasson@tect.co.za.

https://doi.org/10.1016/j.tecto.2018.11.004
Received 4 April 2018; Received in revised form 1 November 2018; Accepted 12 November 2018
Available online 16 November 2018
0040-1951/

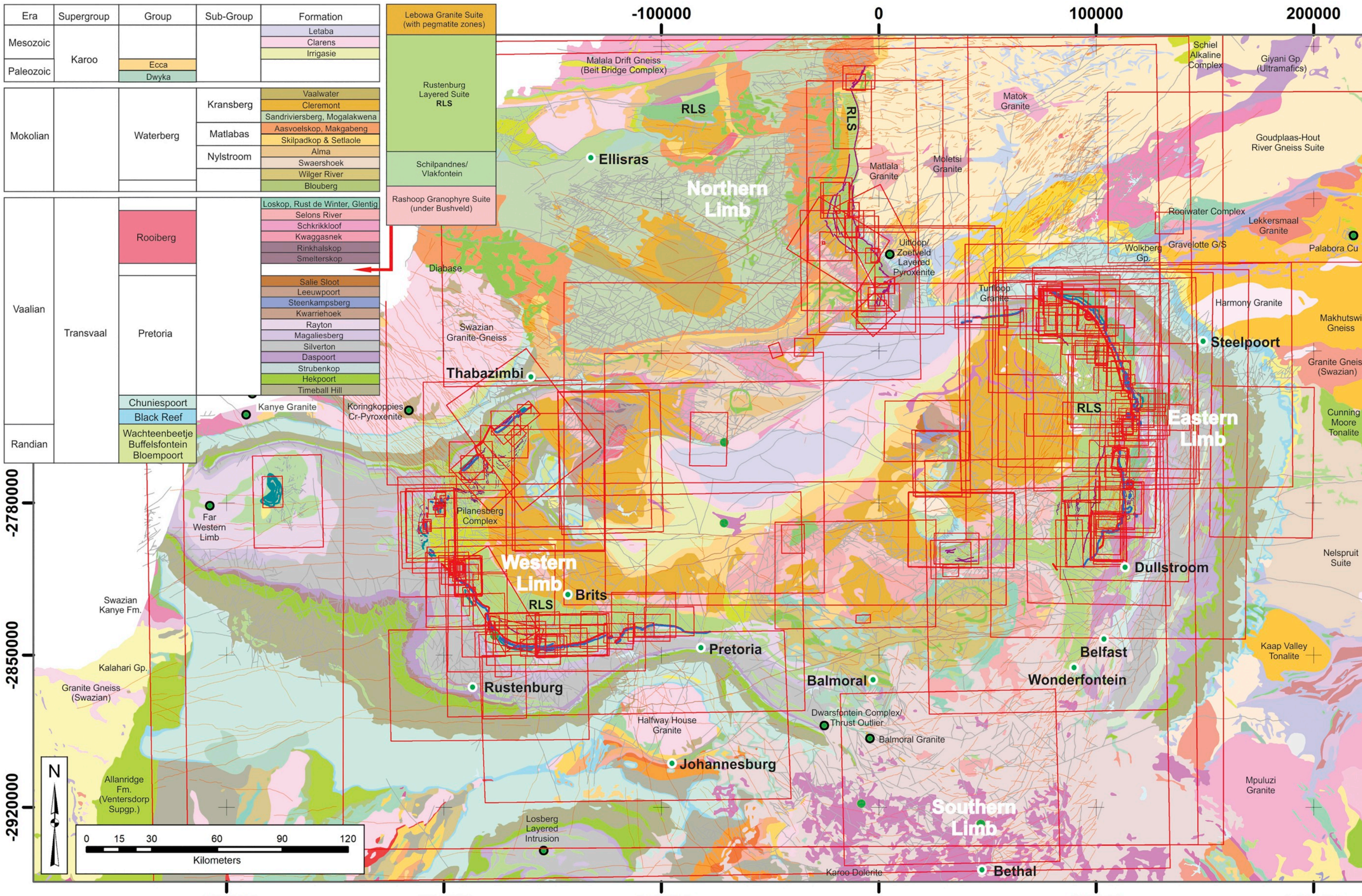

Fig. 1. The Bushveld Complex, showing its four main limbs: Eastern, Western, Northern and Southern, according to the open-source Council for Geosciences' ArcMap project (lithologies only; Geological Survey of South Africa (1974, 1978a, 1978b, 1981, 1985)). The legend is generated for this study and applies to all subsequent figures. The map and legend also highlight the Transvaal Supergroup and Waterberg Group, while older basement units are labelled individually. A fifth limb, termed the Far Western Limb occurs to the west of the Western Limb. The outlines of 254 public-domain maps and figures, from 154 publicly-available articles and reports, are shown and are listed in ancillary data. All figures are in Hartebeesthoek 1994, Lo 29.

topography and structure of the underlying sedimentary basin (Cawthorn et al., 2006). This zone is characterized by cumulate pyroxene and olivine-rich layers, including pyroxenite and harzburgite (Viljoen and Schurmann, 1998).

The Critical Zone, characteristically subdivided into Upper and Lower parts, occurs primarily in the Western and Eastern Limbs. The first occurrence of cumulus chromite marks its base, while the poikilitic Giant Mottled Anorthosite occurs several meters above the well-known Merensky Reef, near the top of the Critical Zone. Both the Lower and Upper Critical Zones display well-defined layering and exhibit enrichment in PGEs and chromite (Cawthorn et al., 2006), compared to marginal cumulates (Cousins, 1959; Vermaak and Von Gruenewaldt, 1986; Viljoen and Schurmann, 1998). The Lower Critical Zone comprises orthopyroxenite, harzburgite and chromite layers while the Upper Critical Zone contains chromite, feldspathic orthopyroxenite, norite and anorthosite/troctolite layers (Kruger, 2005). Chromite stringers or layers are typically subdivided into three groups: Lower Group (LG), Middle Group (MG) and Upper Group (UG; Cousins and Feringa, 1964; Viljoen and Schurmann, 1998). The complex is significant in a global economic context; for instance, Cawthorn (1999) cited 939 Moz of Pt and 711 Moz of Pd, to depths of 2 km, representing 75% and 50% of the world's resource for these metals, respectively. Chromite layers that host these high-value PGMs also host 45% of the world's chromium resources, according to Cawthorn et al. (2005).

The Main Zone is a thick succession of pyroxenite, anorthosite and norite/gabbronorite (Cawthorn et al., 2006). Notable markers include the Pyroxenite Marker and the Main and Upper Mottled Anorthosite (Eales and Cawthorn, 1996). Upper Zone gabbronorite and anorthosite with cumulus Fe-rich pyroxenes, olivine, magnetite and apatite contain numerous V-bearing (Cawthorn et al., 2006) magnetite stringers (Eales and Cawthorn, 1996). In the main body of the complex, the RLS either shallowly cross-cuts the upper Pretoria Group or follows its contact, with the later Lebowa and Rashoop Suite granites intruding into the upper portions of the RLS and Rooiberg felsites (Eriksson et al., 1995).

Much of the current debate and research on the complex centers around: a) the geometry in the central portion of the main chamber; b) historical or present continuity between the complex's various limbs and c) emplacement mechanism(s) and feeders. This study summarizes the cumulative effects of syn- to post-intrusion deformation of the Bushveld Complex and presents an updated suite of data, reports and literature to demonstrate that the original geometry of the Bushveld Complex was very different from its current geometry. This analysis is based primarily on a revised structural interpretation of the complex, combined with an overview of key observations from the scientific literature and competent person's reports on current mining and exploration operations. The current state of knowledge of the complex's macro-scale geometry and connectivity at depth, based on 3D gravity inversion work by Cole et al. (2013), Finn et al. (2015) and others, is considered. An unconstrained inversion of regional gravity and aeromagnetic data was undertaken and is discussed in the context of the reinterpreted fault and dyke network and “out-of-place” or anomalous occurrences of RLS. The study concludes with a suggestion of the complex's geometry prior to the bulk of its deformation, which will contribute to ongoing research on resolving the complex's 3D geometry, particularly geophysical data inversion studies and exploration efforts for PGEs and chromite.

2. Satellite complexes

Early studies (Hall, 1932; Willemse, 1969 and Hunter, 1976) identified a series of related or “satellite” intrusions, many of which are of a similar age to the Bushveld Complex (Fig. 1; Ernst, 2014). These were initially identified as the Far Western Limb; the Crocodile Pools granite and the Modipe gabbro in the vicinity of the Kanye Granite; the Balmoral Granite (now grouped with the Nebo, Lease, Bobbejaankop, Verana, Mukutso and Klipdrif Granites of the Lebowa Suite; Fig. 1); the Dwarsfontein-Nooitgdacht Complex near Argent; the Losberg Layered Intrusion; the Uitloop/Zoetveld layered pyroxenite body; the chromitiferous pyroxenite at Koringkoppies and the Phalaborwa Complex to the east of the Bushveld Complex. The extent of these satellite bodies and the metamorphic aureole of the Bushveld Complex (Sharpe and Chadwick, 1982; Wallmach et al., 1989; Harris et al., 2003; Buick et al., 2004; Longridge et al., 2009), demonstrate that the Bushveld Complex's intrusion affected a significant portion of the Kaapvaal Craton.

3. Age of the Bushveld Complex

Several early articles focused on the age and crystallization time of Bushveld Complex magma. For example, Cawthorn and Walraven (1998) calculated that the entire complex had cooled to < 900 °C after 180,000 years - assuming a solidus temperature of ~900 °C - thereby completely crystallizing in 200,000 years. Uken et al. (2003) cite Harmer and Armstrong (2000)'s SHRIMP ages for the crystallization of the Rooiberg Group, RLS and LGS. These ages are essentially indistinguishable and it was proposed that the entire phase of magmatic activity occurred within 3–5 Myr. Buick et al. (2001) proposed that the RLS was emplaced between 2059 and 2061 Ma. Gerya et al. (2004) studied the formation of the Phepane Dome, concluding that its formation as a diapir within hotter mafic units took < 1 Myr. These results are largely supported by later studies, such as Potter (2009), who estimated between 2 kyr and 2 Myr for the formation of the Phepane Dome as a rising diapir, based on O and Li isotopic compositions and diffusion across the dome's contacts. More recently, Zeh et al. (2015) concluded that emplacement of the complex occurred in < 1 Myr (see also Cheney and Twist, 1991). These models broadly support older palaeomagnetic measurements (e.g. Hattingh, 1986), which suggest that layers of the Main Zone, believed to have crystallized from the youngest magmatic pulse (Sharpe, 1985), were still horizontal when they cooled through their Curie temperature. Mungall et al. (2016) proposed that the complex developed in a series of out-of-sequence sills. In summary, the intrusion and cooling of the bulk of the Bushveld Complex and most of its satellite intrusions, took place in a geologically short space of time.

4. Overview of structural studies

Despite its size and extent, the syn- and post-intrusion deformation of the Bushveld Complex has been relatively poorly addressed in the literature, compared to an extensive body of work on its mineralogy, mineralization and geochemistry. Overviews and observations regarding its intrusion mechanism, its effect on country rocks and post-intrusion deformation may be found in Hall (1932), Truter (1955), Kent (1957), Brock (1957), Cousins (1959), Worst (1959), Verwoerd (1963), Willemse (1959, 1964, 1969), Hunter (1975, 1976), Vermaak (1970), Walraven (1974), Walraven and Darracott (1976), Coetzee (1958, 1970), Molyneux and Klinkert (1978), Von Gruenewaldt (1979), Sharpe and Chadwick (1982), Hartzer (1987, 1995), Du Plessis and Clendenan (1988), Engelbrecht (1988), Bumby et al. (1998), Uken (1999), Du Plessis and Walraven (1990), Walraven et al. (1990), Carr et al. (1994), Good and De Wit (1997), Uken and Watkeys (1997a, 1997b), Martin (1999), Webb et al. (2004), Clarke et al. (2000, 2005, 2009), Greyvensteyn (2001), Nex (2005), Alexandre et al. (2006), Letts et al. (2009, 2011), Finn et al. (2015) and Bamisaiye et al. (2017).

The other *a priori* observation regarding historical studies, with the possible exception of work by Hunter (1975), Hunter and Hamilton (1978)), Von Gruenewaldt (1979), Sharpe and Chadwick (1982), Hartzer (1987, 1995), Walraven et al. (1990), Du Plessis and Walraven (1990); Uken and Watkeys (1997a, 1997b), Cawthorn et al. (1998), Uken (1999); Cawthorn and Webb (2001), Van der Merwe (2007), Clarke et al. (2009), Cole et al. (2013) and Finn et al. (2015) is that the structural and deformational history of the complex has been addressed either piecemeal, such as the relatively well-researched northern margin of the main complex, by relating intrusion events to deformation events (e.g. Carr et al., 1994; Cawthorn et al., 1998; Cawthorn and Webb, 2001), by discussing the effects of major lineaments and their trends and timing (Walraven et al., 1990; Good and De Wit, 1997; Bamisaiye et al., 2017) or through petrographic and geochemical studies that describe igneous stages or events in the complex's development (e.g. Cawthorn et al., 1991; Van Tongeren and Mathez, 2009; Van Tongeren et al., 2010; Wilson, 2012, 2015; Wilson and Chunnett, 2010; Mathez et al., 2013; Cawthorn, 2013; Zeh et al., 2015; Ireland and Penniston-Dorland, 2015; Maier et al., 2016; Huthmann et al., 2016; McDonald et al., 2017; Hayes et al., 2017a).

Transvaal Supergroup deformation was related by Visser (1957) to the emplacement of the complex while Cousins (1959), Liebenberg (1970) and Vermaak (1970) essentially supported the view that deformation preceded the complex's intrusion and that any strain or folding effects were merely due to the subsidence of the encompassing sedimentary basin. Regional geological mapping by Schwellnus (1956), Schwellnus et al. (1962) and Bastin (1968) provided evidence for large fold structures and large country rock xenoliths in the floor of the complex. Tectonic fabrics and signs of dynamic metamorphism were recorded by Button (1973) and Blain (1975), particularly bedding-parallel fabrics in Pretoria Group pelites. Walraven (1981) noted that Transvaal Supergroup units within the vicinity of the complex are "relatively undeformed and display the original basin shape rather well".

While Schwellnus et al. (1962) proposed that strike-slip faulting along the Wonderkop Fault was both post-Bushveld Complex *and* post-Waterberg Group, Miyano et al. (1987) attributed all deformation in the Mohlapitsi Fold-and-Thrust Belt to a much younger, post-Waterberg Group event. Deformation of the Waterberg Group is characterized by open folds, predominantly to the south of the Thabazimbi-Murchison Lineament (TML; see Figs. 4 and 5), with the most intense deformation flanking this lineament. Meinster (1974) attributed deformation along the TML to northward-directed thrusting and associated folding, whereas Du Plessis (1987) proposed a positive flower structure caused by left-lateral movement in post-Pilanesberg times (*c.* 1.3 Ga; see Martin et al., 1988). Du Plessis and Walraven (1990) proposed a regional strike-slip tectonic model for the Bushveld Complex, including pre-Bushveld Complex right-lateral movement in the TML to produce the Mohlapitsi Fold-and-Thrust Belt, considered by most of the earlier studies as being unrelated to Bushveld Complex-aged tectonism (e.g. Schwellnus et al., 1962; Bastin, 1968; Button, 1973; Miyano et al., 1987). Du Plessis and Walraven (1990) also proposed that the Mohlapitsi Fold-and-Thrust Belt pre-dates the pre-Pretoria Group unconformity. Left-lateral reactivation of the TML, with associated N- to NW-trending, en-echelon folding, attributed to gravity inversion tectonics in the floor of the complex, was proposed by Du Plessis and Walraven (1990), who also related this strike-slip movement to the initiation of Waterberg Group sedimentation.

Studies on the Bobejaanswater Fault System (Du Plessis and Clendenan, 1988; see Fig. 4) revealed left-lateral, transpressional fault movement (see also Wilcox et al., 1973; Reading, 1980; Harding, 1985) at approximately 2.0 Ga, supported by mylonitised Bushveld Complex granite within fault zones. These models were summarized by Uken (1999), who suggested that the northern margin of the eastern Bushveld Complex exhibits two main structural trends: a) the abovementioned, ENE-trending Mohlapitsi Fold-and-Thrust Belt, notably affecting the Chuniespoort and Wolkberg Groups (Button, 1973) and large, N–S-oriented or -elongated periclines in the contact-metamorphosed Pretoria Group within the floor of the Bushveld Complex. Potgieter (1991) documented two coaxial fold phases in sub-Pretoria Group units (F_1 and F_2). In their scheme, F_1 folds are northward-verging kink-folds of pre-Pretoria Group age, whilst tight F_2 folds, present only in proximity to the Bushveld Complex, were interpreted as post-Pretoria Group in age but syn-Bushveld Complex intrusion. Uken (1999) cited three main deformation phases a) D_1 - Structures of pre-Bushveld Complex age; b) D_2 - All syn-Bushveld Complex/RLS-age deformation and c) D_3 - Post-Bushveld Complex deformation.

The TML is consequently a well-studied, major tectonic boundary with a cumulative vertical displacement of approximately 10 km and an overall left-lateral or sinistral displacement of 8–10 km, according to Good and De Wit (1997). The TML, along with the Bobejaanswater Fault System, Mohlapitsi Fold-and-Thrust Belt, the Welgevonden/Southern Fault System and the Zebedelia Fault, collectively acted as a broad, anastomosing and/or relay structure with overall left-lateral, transpressional shear during and after emplacement of the complex. The abovementioned studies do not, however, extend very far southwards into the main chamber of the complex, where signs of deformation include steepened cumulate layering around domes or adjacent to major faults, such as the Steelpoort, Rustenburg and Crocodile River Faults (see Fig. 4), deformation adjacent to preserved country rock fragments, the effects of domes, "anomalous" RLS intersections in mining and exploration projects, and regional magnetic or seismic data. In terms of the complex's overall geometry at depth, Cheney and Twist (1991) concluded that the complex and its enclosing strata are "synformally folded" into a lopolithic form.

Domal structures are present in high-grade metasedimentary units within the complex's aureole (e.g. Hartzer, 1995; Uken and Watkeys, 1997a; Uken et al., 2003; Johnson et al., 2004; Lenhardt and Eriksson, 2012). Broadly speaking, domes disturb the footwall or lower contact and penetrate the RLS to various extents. Hartzer (1995) discussed the Dennilton, Marble Hall and Makeckaan/Stavoren Domes/Fragments that are attached to the floor or basal sedimentary succession. Uken and Watkeys (1997a) refer to at least seven large diapirs or diapiric structures, of contact-metamorphosed Pretoria Group sediments, which penetrated the overlying RLS, while Greyvensteyn (2001) lists a total of fifteen "inliers" of various classes, including domes, diapirs, xenoliths and fragments. According to Uken et al. (2003), diapirs developed above a décollement that corresponds to the 550 °C metamorphic isotherm (Uken and Watkeys, 1997a), while Johnson et al. (2004) proposed a characteristic spacing of 20–40 km and wavelengths of several kilometres for domal structures. Button (1973, 1976), proposed that domes are diapiric in nature, a concept elaborated upon by Clarke et al. (2009) who suggested a finger-like intrusion of the lower parts of the layered suite and diapir formation by magma loading and ductile, upwards amplification of underlying floor rocks. Johnson et al. (2004) attributed spinel-cordierite symplectites, which replaced andalusite within migmatitic or migmatized units within the cores of domes, to decompression during melt-assisted diapirism (see also Gerya et al., 2003). The origin of these asperities has been extensively debated in the literature and has been the subject of modelling and computer simulations; however, most studies seem to attribute them primarily to pre-RLS folds or asperities that were enhanced or accentuated by the emplacement of the mafic-ultramafic portion of the complex (e.g. De Waal, 1970; Sharpe and Chadwick, 1982; Du Plessis and Walraven, 1990; Hartzer, 1995; Uken and Watkeys, 1997a; Bumby et al., 1998).

Several key observations from these studies are discussed later in this contribution; however, the vast majority of early work views the complex as "static". In other words, the predominant view on the complex has been that its current geometry, shape or coverage was essentially established at the time of its intrusion and that any observable deformation features, including that within the host Transvaal Supergroup, were either: present at the time of intrusion; due to further basin subsidence; caused by heat imposed by the complex's intrusion or concentrated along the northern margin of the main chamber.

5. Data types and coverage

Most studies on the Bushveld Complex reproduce a series of regional 1974–1986 1:250,000 scale maps, issued by the Council for Geoscience (2328 Pietersberg; 2330 Tzaneen; 2526 Rustenburg; 2528 Pretoria; 2530 Barberton; 2626 Wes-Rand; 2628 East Rand; 2426 Thabazimbi;

2428 Nylstroom; 2430 Pilgrims Rest). These maps also reflect a regional map published and discussed by Hunter (1975, 1976), Walraven (1989) and Hunter and Hamilton (1978). Greyvensteyn (2001), in an unpublished thesis, re-digitized Council for Geoscience maps and undertook a revised lineament analysis of major structures; however, this data set was not available at the time of writing. A revised 2008 map of the Eastern Limb was made commercially available by T.G. Molyneux, in collaboration by M. Frei. This built upon work of Molyneux (1974), Molyneux and Klinkert (1978) and a number of observations from personal mapping, literature and archives at the Department of Geology, University of Pretoria. This compilation contains only a handful of structures and is primarily focused on the finer detail of cumulate layering. South Africa's Council for Geoscience released an ArcMap vector version of lithologies and several larger major structures, which, combined with a handful of selected lithological elements from the Molyneux (2008) compilation, is used as a contextual backdrop to the revised interpretation provided herein, although structures have been extensively re-interpreted and updated for this contribution.

A significant amount of work has been undertaken by researchers, exploration companies and mining companies, often in concert. The great majority of this work is mineralogical or geochemical in nature; however, the most accessible and useful information pertaining to the geometry and structure of the complex is presented in technical and competent person's reports produced by mining and exploration companies and in compiled geophysical data by, for example, Cole et al. (2013), Webb et al. (2004), Webb et al. (2011) and Finn et al. (2015). A total of 254 maps and figures from 154 open-source reports and published articles were georeferenced (Fig. 1) and superimposed on a high-resolution SRTM backdrop. Due to the focus on surficial or near-surficial, economically-viable areas, most of the detailed maps and local geophysical data sets are concentrated over the Eastern, Western and Northern Limbs. Each map was georeferenced and catalogued using standard database fields, such as source/author, publication date and figure number within the source publication. Structural features and reef positions (UG2, Merensky, LG and MG chromitites, magnetite reefs; $N = 842$ segments) were digitized and merged with adjacent and overlapping data. Components of the revised interpretation include faults ($N = 10{,}130$ segments), dykes ($N = 5{,}116$ segments), fold axes ($N = 184$), bedding and tectonic fabrics ($N = 25{,}722$ short linear elements), orientation data ($N = 5{,}396$ readings), dunite pipes and iron-rich ultramafic pegmatoids (IRUPs) and iron replacement bodies ($N = 3{,}189$; see also Scoon and Mitchell, 1994; Reid and Basson, 2002; Smith and Basson, 2006). Other features of interest include domes, diapirs, xenoliths, fragments and periclines (Hartzer, 1995; Greyvensteyn, 2001), geophysical anomalies, sills, proximal satellite complexes, grabens, troughs, “bulges” and kimberlites ($N = 725$). In addition to this, major deposits, shafts, declines and adits were also demarcated and are occasionally employed as positional references in the following analysis (Fig. 2). Where represented or interpreted from drillhole data in technical reports, UG2 and Merensky Reef contours ($N = 868$), with their tagged depths below an average surface or their elevations relative to sea level, were extracted from georeferenced figures.

6. General structural geometry

A general overview of the shape of the complex, with the aid of the revised structural interpretation (Fig. 2), shows several key features, the foremost of which is the general mode of deformation and kinematics within the three dominant limbs (Eastern, Western and Northern) and the central part of the main chamber. Key features and offsets are highlighted in the following sections.

6.1. Eastern Limb

The northern portion of this limb is effectively absent or undetected to the west of Messina Platinum Mine (Fig. 3). This area is occupied by basic volcanic units (tholeiites, picrite basalts and nephelinites) and augen quartz-feldspar gneiss. A regional reflection seismic survey over the north-eastern Bushveld Complex, acquired by the Geological Survey of South Africa, traverses the Transvaal Supergroup and the Bushveld Complex (Odgers and du Plessis, 1993). Several major structural features were resolved from this, including the Wonderkop Fault System, the Phepane/Paradys and Lezwete Structures and the Malope Dome(s). The northern portion of the limb, to the east of Messina Platinum Mine, hosts a series of NE-trending left-lateral faults, including the Wonderkop (Odgers and du Plessis, 1993) and Stofpoort Faults. This left-lateral displacement appears to be progressively greater from east to west. These structures displace the RLS left-laterally and are paired by conjugate, short strike-length, NW-trending, right-lateral, strike-slip faults. There is a notable steepening of dip (up to 60°; see stereonets a, b and c of Fig. 3; all stereonets are equal area, lower hemisphere) of the cumulate layering towards the Zebedelia Fault and the northern edge of the Eastern Limb. This area is also remarkable due to generally tight folding and steepening of the local tectonic fabric, including that within the Mohlapitsi Fold-and-Thrust Belt (Miyano and Beukes, 1987) and the Murchison Belt to the east (e.g. Jaguin et al., 2012).

The complex to the south and down-dip contains a series of domes, summarized in Hartzer (1995) and Greyvensteyn (2001). These include the Adriaanskop Dome (Johnson et al., 2004); the Malope Dome(s) (Odgers and du Plessis, 1993; Johnson et al., 2004); the Schwerin Floor Dome (Uken, 1999; Clarke et al., 2009); the Zaaikloof/Phosiri (=M'Phatlele/Fontdraai) Dome (Hartzer, 1995; Uken, 1999; Schweitzer et al., 2009); the Katkloof Dome/structure (Hartzer, 1995; Uken, 1999); the Phepane/Paradys Dome (Odgers and du Plessis, 1993; Uken, 1999; Scoon, 2002; Johnson et al., 2004); the Signal Hill/Boschpoort/Makgane Dome (Schweitzer et al., 2009); the Elandslaagte Dome (Hartzer, 1995); the Dennilton Dome (Clubley-Armstrong and Sharpe, 1979; Hardwick et al., 2015); the Schwerin Structure (Hartzer, 1995; Uken, 1999) and numerous other minor domes, structures, fragments, anticlines and periclines. ENE-trending folds (see stereonets f and i of Fig. 3) and these domes, many of which are addressed and/or modelled in Hartzer (1995), Uken (1999), Gerya et al. (2004) and Clarke et al. (2009), are effectively contained within the Burgersfort Bulge, a convex-east, apparently NE-impinging, portion of the Eastern Limb (Fig. 3). This feature is bound to its north by the extensive Wonderkop Fault and its associated Stofpoort Fault splay, and constrained to the south by the extensive, anastomosing Steelpoort/Dwarsrivier Fault system (Clarke et al., 2005), which shows ductile, right-lateral offset. The eastward “impingement” of this part of the complex is supported by structural studies on deposits that occur up to 110 km further eastwards of the complex. These exhibit eastward-verging, low-angle thrusting in Au mines to the north of Pilgrim's Rest (Molyneux and Klinkert, 1978; Harley and Charlesworth, 1992, 1993, 1996; Boer et al., 1995; Tyler and Tyler, 1996; see also Rasmussen et al., 2007) and locally eastward-directed, Bushveld-aged stress during the final stages of mineralization at Palabora Copper Mine (Basson et al., 2017). The complex displays very localized folding and southward-directed thrusting to the south of the Steelpoort/Dwarsrivier Fault and a second, but comparatively minor “bulge”, with its northern margin near the Two Rivers Platinum Mine and its southern margin along the right-lateral Laersdrif Fault System. Broad folds, expressed by outcrops of granite and rhyolite, tend to follow the trends of the abovementioned major faults; however the complex and its host Pretoria Group are comparatively flat-lying to the south-east of the Burgersfort Bulge (stereonets j and k of Fig. 3).

6.2. Western Limb

The Western Limb is possibly better studied, compared to the other limbs of the complex, due to protracted and typically deeper mining operations and its relatively flatter topography. In the north, the limb

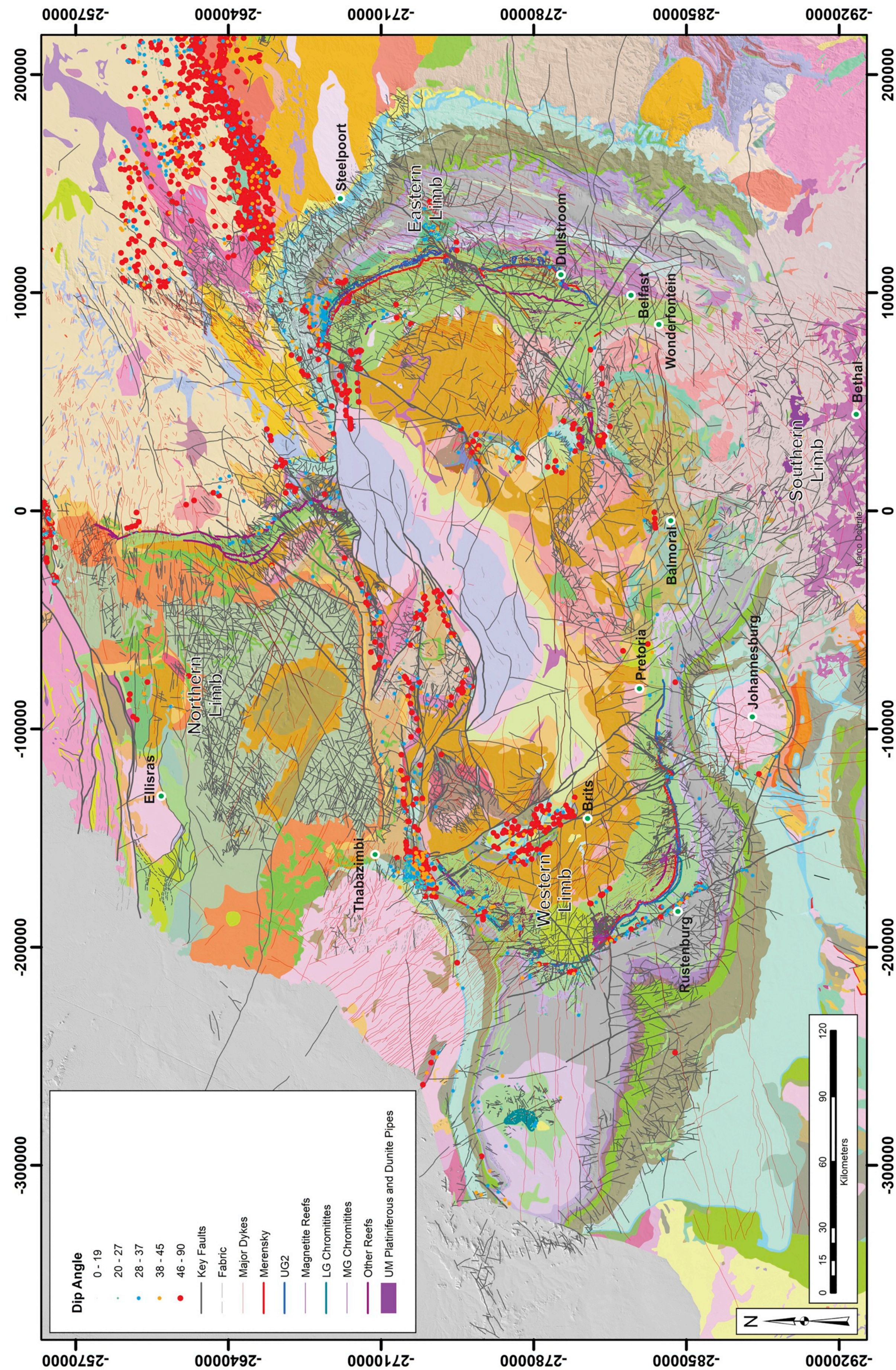

Fig. 2. Detailed structural interpretation, based on the compiled and georeferenced maps referred to in Fig. 1, with a backdrop of the Council for Geosciences' ArcMap project (lithologies only). Strike and dip symbols have been reduced in size and displayed as colour-coded dips to avoid cluttering.

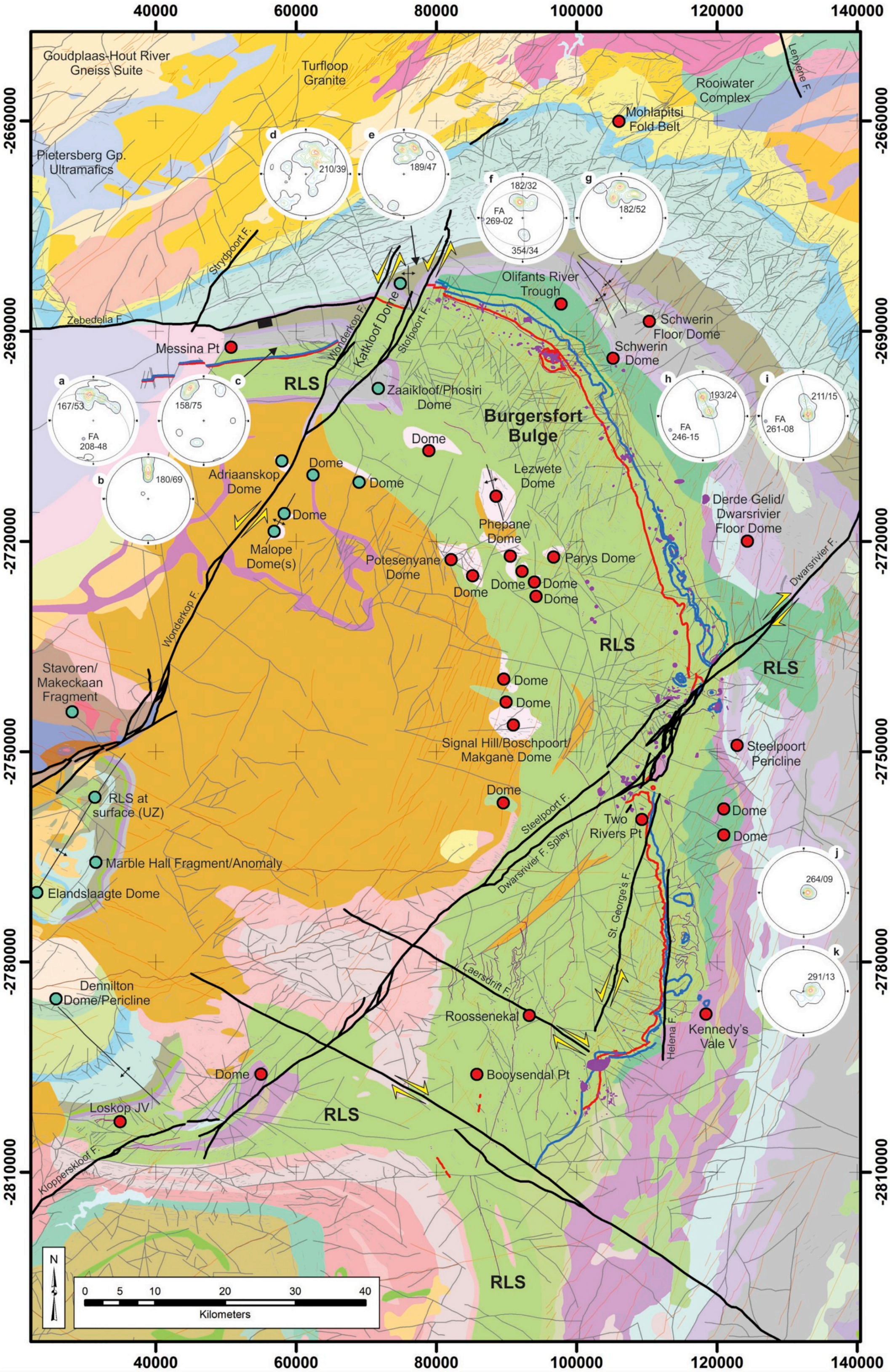

Fig. 3. Detailed map of the Eastern Limb of the Bushveld Complex. The Eastern Limb, in particular the Burgersfort Bulge, contains a disproportionate number of domes or periclinal features, compared to the remainder of the Bushveld Complex. Intense folding and high strains are evident along its northern margin. Compilation of structural data west of the Wonderkop Fault, in the Messina Pt area: a) bedding at Av = 167°/53° (CGS, $N = 31$; Uken, $N = 52$) with a derived fold axis of 208°–48°; b) cumulate layering at Av = 180°/69° (CGS, $N = 20$) and c) S_{2a} planar foliation at Av = 158°/75° (Uken, $N = 38$); Praamkoppies Domain: d) bedding at Av = 210°/39° (Uken, $N = 116$) and e) S_{2a} planar foliation at Av = 189°/47° (Uken, $N = 28$); Mathabatha Domain: f) bedding at Av = 182°/32°; 354°/34° with a derived fold axis of 269°–02° (Uken, $N = 120$) and g) S_{2a} planar foliation at Av 182°/52° (Uken, $N = 62$); Burgersfort Bulge: h) bedding at Av = 192°/24° with a derived fold axis of 246°-15° (CGS, $N = 119$) and i) cumulate layering at Av = 211°/15° and a derived fold axis at 261°-08° (CGS, $N = 123$); South-east of the Burgersfort Bulge: j) bedding at Av = 264°/09° (CGS, $N = 93$) and k) cumulate layering at Av = 291°/13° (CGS, $N = 242$).

apparently terminates against the right-lateral Crocodile River Fault, extending for at least 130 km to the south, which bounds the Crocodile River Dome or Fragment on its eastern side (Jansen et al., 1974; Walraven, 1981; Hartzer, 1995). This fault is paralleled, to its west, by a series of NNW-trending, right-lateral faults, most notably the Brits Graben Fault, Hartebeespoort Fault and the Bokfontein/Roodekoppies Fault further southwards (Fig. 4). The Hartebeespoort Fault system notably offsets the UG2 and Merensky Reefs in the Krokodildrift/

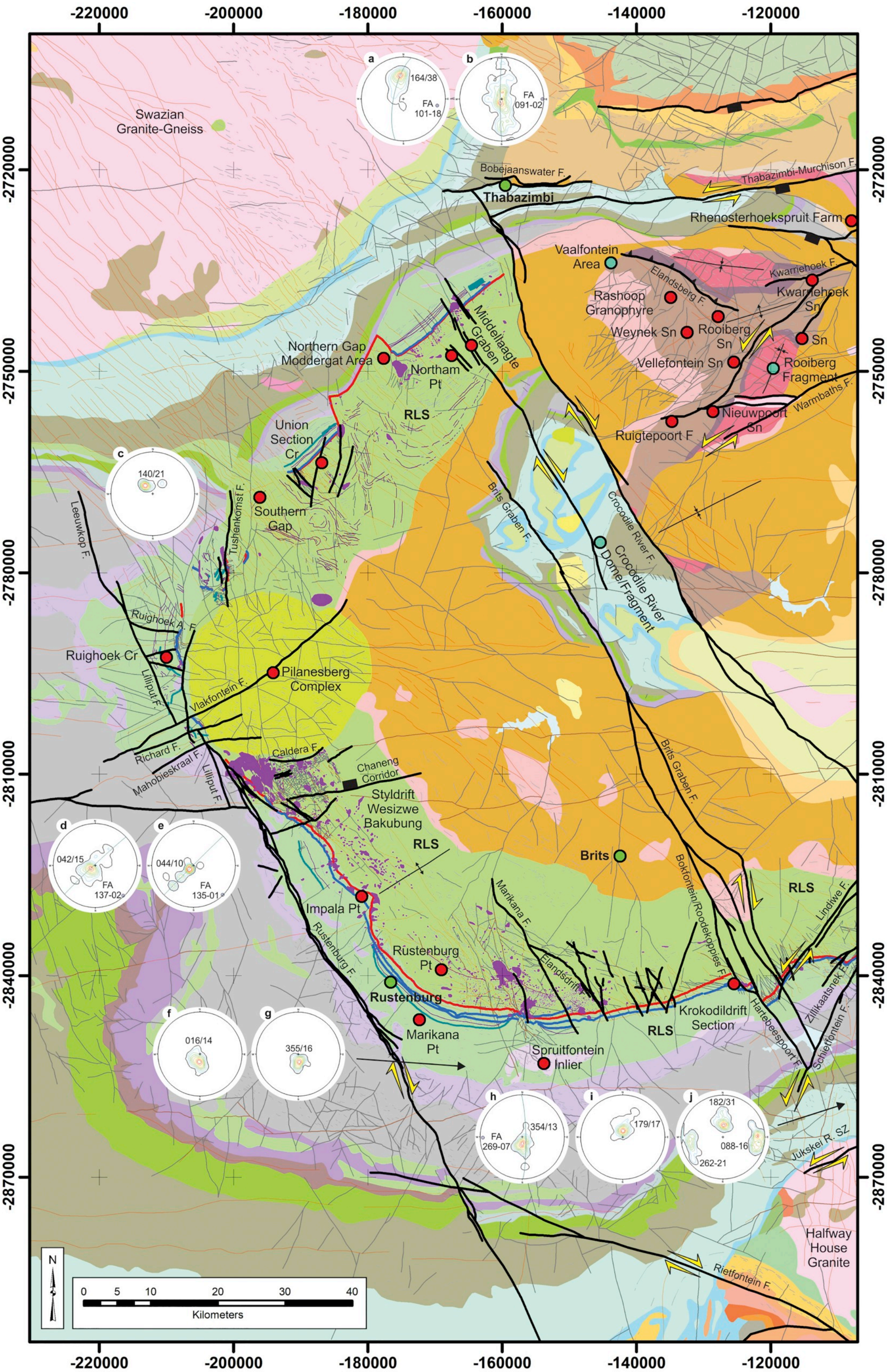

(caption on next page)

Fig. 4. Detailed map of the Western Limb of the Bushveld Complex. Key features include: significant N-up reverse faulting along the Thabazimbi-Murchison Lineament, Zebediela, Planknek, Welgevonden/Southern, Bobejaanswater Fault system(s); SSE-directed thrusting in the Droogekloof Thrust, Boschpoort Fault/Thrust and Southern Boundary Fault system and the development of two "gap areas". The Western Limb differs from the Eastern Limb in several ways: there is an almost complete absence of domes in the Western Limb, although several NNW-trending, right-lateral faults (Crocodile River, Middellaagte and Brits Graben Faults) have contributed to uplifted units within the Crocodile River Dome/Fragment. Another unique feature is gap areas, with margins that are effectively parallel to the abovementioned faults, and a plethora of IRUPs, particularly to the south of the Pilanesberg Complex. Compilation of structural data in the Thabazimbi area: a) bedding at Av = 164°/38° with a derived fold axis at 101°–18° (CGS, Boardman, N = 586) and b) planar, fanning, fold axial cleavage distributed around 091°-02° (CGS, Boardman N = 234); Northern part of Western Limb: c) cumulate layering at Av = 140°/21° (CGS, N = 86); South of Pilanesberg Complex: d) bedding at Av = 042°/15° with a derived fold axis of 137°-02° (CGS, N = 133) and e) cumulate layering at Av = 044°/10° with a derived fold axis at 135°-01°; southern part of the of the Western Limb in the Rustenburg area: f) bedding at Av 016°/14° (CGS, N = 86) and g) cumulate layering at Av 355°/16° (CGS, N = 40); north of the Johannesburg Dome (all data Gibson et al., 1999): h) bedding at Av = 354°/13° with a derived fold axis at 269°–07° (N = 69); i) cleavage at Av = 179°/17° (N = 61) and j) combined axial planes at Av = 182°/31° (N = 34), and doubly-plunging fold axes at 088°-16° and 262°–21° (N = 41).

Zandfontein Section, accompanied by a set of conjugate, NE-trending, left-lateral faults (Dube, 2010). On the western side of the Pilanesberg Complex, the Rustenburg Fault, which has a strike length of at least 125 km, exhibits an identical NNW orientation and right-lateral movement, which continues northwards and to the west of the Pilanesberg Complex in the form of a myriad of small-scale faults that segment the UG2 and Merensky reefs near the Ruighoek Cr Mine (Waldeck et al., 2007). The Transvaal Supergroup to the north of Thabazimbi shows intense folding and thrusting (Basson and Koegelenberg, 2017; stereonets a and b of Fig. 4).

The Western Limb differs from the Eastern Limb for several reasons. Firstly, there are distinct reef sub-facies to the north and south of the Pilanesberg Complex, termed the Swartklip and Rustenburg Sub-facies, respectively (Viljoen, 1994, 1999). "Gap areas", wherein Upper Zone units are juxtaposed against Main, Critical and Marginal Zone units, occur between "sections" wherein the normal cumulate sequence is preserved (Wilson et al., 1994; Viljoen, 1999; Reid and Basson, 2002). These gap areas show extensive development of pegmatites, syn- to late-magmatic feldspathic veins and iron-rich ultramafic pegmatoids (Lee, 1981; Viljoen and Scoon, 1985; Scoon and Mitchell, 1994; Reid and Basson, 2002). Examples of these include the Moddergat area along the south of Anglo's Amandelbult Section and in the Northern Gap area, and the Southern Gap area south of Union Section. The Pilanesberg Complex occurs at an inflection between the northern and southern parts of the Western Limb. In this respect, its position is similar, or analogous, to the Roodeplaat Complex, which also occurs at an inflection in the complex, where the UG2 and Merensky reefs apparently terminate. The RLS to the south of the Pilanesberg Complex, based on high-resolution, public-domain aeromagnetic images over the Styldrift/Wesizwe/Bakubung property, displays a dense network of conjugate, NE- and NW-trending faults, fractures and alkaline dykes, accompanied by severe intrusion of and/or alteration by iron-rich ultramafic bodies. This suggests a zone of locally very high strain due to the southward impingement of the Pilanesberg Complex.

Bedding and cumulate layering are folded about NW-SE-trending axes (stereonets d and e of Fig. 4), while around the south-western "elbow" of the Western Limb, bedding and cumulate layering are comparatively flat-lying (stereonets f and g of Fig. 4). The UG2 and Merensky reefs of the Western Limb terminate, in their southern extremities, east of the Krokodilkraal/Middelwater area and directly north of the northern apex of the Johannesburg Dome (Gibson et al., 1999), where N- and S-directed, layer sub-parallel to parallel thrusting, axial planar cleavage and ENE-WSW-trending, doubly-plunging folds become dominant (stereonets h, i and j of Fig. 4; see also Clarke et al., 2000). These authors concluded that Chuniespoort Group dolomites and the Black Reef Formation, in the area to the south of the Western Limb and north of the Johannesburg Dome, exhibit evidence of intense bedding-parallel shearing that post-dates Bushveld Complex metamorphism but pre-dates the intrusion of the Pilanesberg Complex. Gibson et al. (1999) attributed this to outward-directed thrusting caused by the 2.03 Ga Vredefort impact event.

6.3. Northern Limb

The Northern Limb (e.g. Van der Merwe, 1978, 1998; Kruger, 2005; Finn et al., 2015; Kinnaird et al., 2005; Kinnaird et al., 2017) is often viewed as a distinct feature, mainly due to its different position in the host stratigraphy, compared to the complex's main body or chamber, and its transgression across underlying Archaean granite-gneiss basement. It contains the Northern Limb (*sensu stricto*) and Villa Nora Segment (Fig. 5) wherein Upper Zone units prevail, with Main and Critical Zones occurring only in the limb's southern extent. The exploited Platreef occupies the base of the northern limb and is considered stratigraphically equivalent to the Critical Zone (Kinnaird and McDonald, 2005; Kinnaird et al., 2005; Kinnaird et al., 2017). Lower Zone rocks are preserved as individual ultramafic bodies (Van der Merwe, 2008). The overall dip of the Northern Limb flattens towards the west (Van der Merwe, 1976), while the Villa Nora Segment, which shows southward dips (Brandl, 1986), consists of gabbro, anorthosite, ferrogabbro and norite of the Upper Zone (Brandl, 1986), although some researchers suggest that Main and Upper Zones are also present (e.g. Kruger, 2005). With fragments inferred from gravity data to the east of the Glenover Complex (Finn et al., 2015), these features collectively form the remnants of a deformed, inward-dipping intrusive body. The northern portion of the Northern Limb, based on regional geophysical data (Finn et al., 2015), is convex-south, mimicking the geometry of the convex-south, southward-verging thrusts and reverse faults that run through the Union Tin Mine (Fig. 6) and Zwartkloof Fluorspar Mine, expressed by locally steepened dips in sedimentary layering.

The relatively well-documented and better-preserved eastern portion of the Northern Limb is gently-folded, suggestive of N–S or NNW–SSE compression with a large-scale "ptygmatic" geometry (Fig. 5). This geometry is accomodated by numerous NE-trending, left-lateral shears and faults that are evident in regional geophysical and remote sensing datasets and detailed pit mapping (Bye and Bell, 2001; Bye and Mossop, 2005), such as the Ysterberg-Planknek Fault, which runs into the TML to the south, the Rooisloot/Mahopane Fault, the Ditlokeng Fault, the Sandsloot Fault and Pruizen (Transcurrent) Faults. Bedding shows local folding about NE–SW trending axes, parallel to these faults. Cumulate layering is WSW-dipping, while axial planar foliation is distributed about an almost due E–W trending fold axis (stereonets a, b and c of Fig. 5). The Northern Limb is also dissimilar due to its separation from the main chamber by a network of linked, offset or anastomosing, ENE-trending, oblique reverse, left-lateral faults, such as the TML, Zebediela, Welgevonden/Southern Faults and the Bobejaanswater Fault system(s) (Figs. 3, 4, 5). Key within this system is the TML, which formed at *c*. 2.7 Ga due to the collision of the Pietersberg and Kaapvaal terranes (Good and De Wit, 1997), and which has been active until recently. Kinnaird and McDonald (2005) suggested that the TML exercised at least some control over the structure of the Bushveld Complex's chamber and the injection of magma at *c*. 2.06 Ga. They furthermore proposed that the TML may have acted as a dyke-like feeder for Bushveld magmas or may have provided a barrier that separated the Northern Limb from the remainder of the complex, possibly resulting in their separate development or evolution. Separate

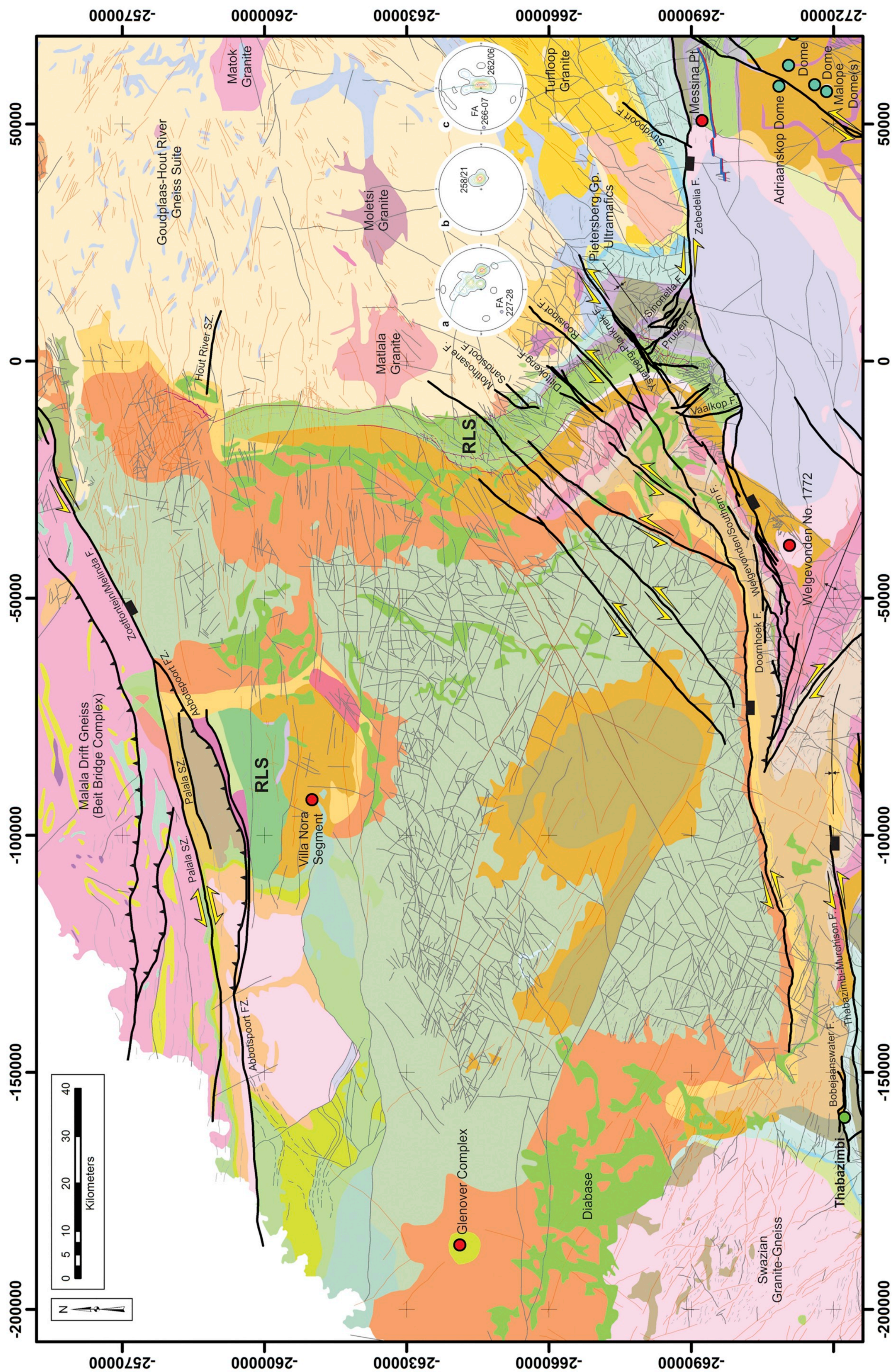

Fig. 5. Detailed map of the Northern Limb. Notable features include the convex-south set of thrusts/reverse faults, showing N-up movement, along the Abbotspoort Fault Zone and Palala Shear Zone in the area of the Villa Nora Segment; predominantly NE-SW trending, left-lateral faults and shears that transect the currently-mined Platreef and a dense network of conjugate faults to the west of this, which collectively suggest S- or SSE-directed compression. Structural data represent a) bedding with a derived fold axis of 227°–28° (CGS, N = 36); b) cumulate layering at Av = 258°/21° (CGS, N = 64°) and c) foliation at Av = 262°/06°, distributed around folds with derived a axis at 266°–07° (CGS, N = 83).

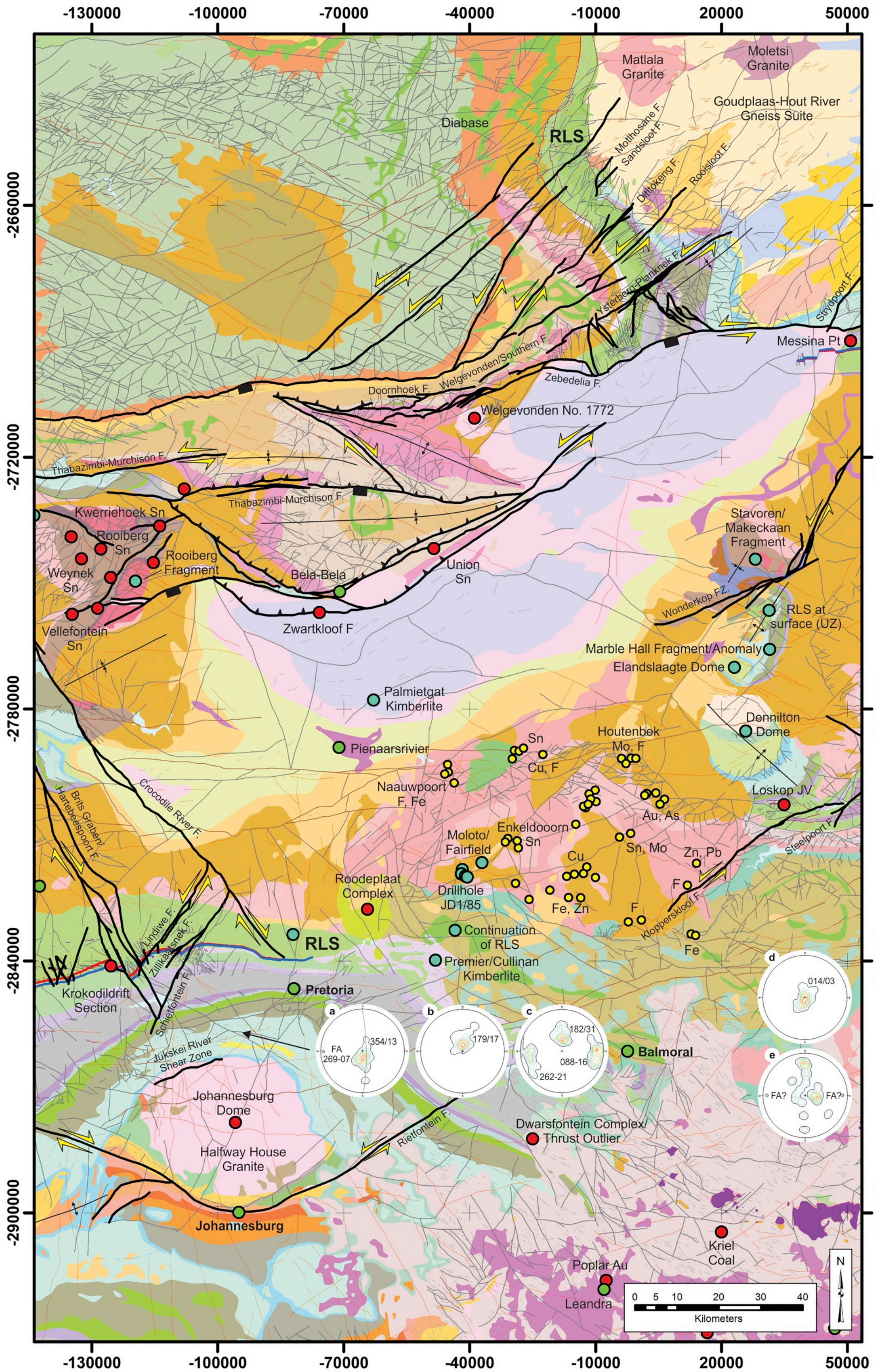

Fig. 6. Detailed map of the central part of the main chamber and the Southern Limb of the Bushveld Complex. Several notable features include a dense cluster of Cu, Fe, Zn, Sn, Mo and F occurrences, very similar to those of the Rooiberg area, within a densely-faulted area dominated by the Lebowa and Rooiberg granophyre and rhyolite, bounded on its SW side by the Klopperskloof-Steelpoort Fault System. The western extent of the central area is bounded by the right-lateral Crocodile River Fault. A series of three en-echelon basins hosting the Ecca, Irrigasie, Clarens and Letaba Formations of the Karoo Supergroup obscure much of the central part. The Southern Limb is largely obscured by Rooiberg Group rhyolite and Vryheid Formation sandstone of the Karoo Supergroup. Stereonets a), b) and c) are identical to stereonets h), i) and j) of Fig. 4. Bedding and cumulate layering to the east of Balmoral are flat-lying to gently folded; d) bedding at Av = 014°/03° (CGS, $N = 74$) and e) cumulate layering with no clearly-defined average and poorly-defined folding about a broadly E–W trending axis (CGS, $N = 23$).

sub-chambers for parts of the Northern Limb were recently proposed by Kinnaird et al. (2017).

The Bobejaanswater Fault or Fault System (Du Plessis and Clendenan, 1988) shows predominantly sub-vertical slickenfibres on its fault planes, although oblique and horizontal fiber growths are also present. The main shear zone is approximately 40 m wide, consisting of ultramylonite with a prominent vertical, planar foliation. Stereonet analysis shows that axial planes and fold axes of small isoclinal folds within the mylonite zone are co-planar with the central fault plane (Du Plessis and Clendenan, 1988). Along with horizontal fold axes, these features are collectively diagnostic of a transpressive fault system (Reading, 1980; see also Jaguin et al., 2012). Indeed, Du Plessis and Clendenan (1988) interpreted a positive flower structure related to left-lateral, transpressive fault movement (see Wilcox et al., 1973; Reading, 1980; Harding, 1985) at approximately 2.0 Ga, an age that is supported by the entrainment of mylonitised Bushveld Complex granite into the fault zone.

6.4. Southern and/or Bethal Limbs

The Southern Limb or Southeastern Limb (Odgers et al., 1993; Kgaswane et al., 2012) of the complex, stretching from Belfast and Wonderfontein in the east (see Hattingh, 1977), through Bethal, to the town of Leandra in the west (Fig. 6), is relatively poorly-documented due to extensive cover by the Karoo Supergroup, a pervasive suite of Karoo dolerite sills and activity on numerous Au and Ag mines (e.g. Bracken, Winkelhaak, Kinross, Leslie, Poplar and Evander) and coal mines (e.g. Kriel). These mitigate against extensive, overlapping exploration for, let alone extraction of, PGEs. Early work by Buchanan (1975) involved petrographic description of the Bethal Limb, which was deemed to comprise the southern extent of the Eastern Limb (see also Van der Merwe, 2007 and Molyneux, 2008), or the partially-connected, easternmost extent of the Southern Limb. While Van der Merwe (2007) re-iterated the presence of the Critical Zone along the exposed "southeastern sector" of the eastern Bushveld Complex, its southwards and westwards extension were inferred from references to Upper Critical Zone intersections near Belfast, drillhole intersections that show geochemical affinities to UCZ near Bethal (Gold Fields of South Africa in the 1970s–80s), several other intersections in deep drillholes and positive gravity anomalies (Hattingh, 1977; Cawthorn and Webb, 2001; Dube, 2010; Cole et al., 2014). However, according to Cawthorn and Webb (2001), it is widely-accepted that only Lower and Upper Zone rocks are preserved, implying that chromitite layers, Merensky Reef and Pyroxenite Marker are not well-developed or are absent (see also Buchanan, 1975). Lonmin Platinum's exploration on its Loskop Joint Venture (Fig. 6) identified several mineralized units, apparently stratigraphically-equivalent to the Upper Critical Zone, with most of the mineralization contained within what is termed the Upper Mineralized Pyroxenite (Harper et al., 2009). In terms of the role of the Southern/Bethal Limb in the genesis of the complex, Kruger (2005) proposed that Upper Zone magma flowed into the main chamber from both the Bethal Limb and the TML, resulting in erosion of Main Zone rocks and regional unconformities, possibly including the gap areas within the Western Limb. Bedding and cumulate layering to the east of Balmoral are flat-lying to gently folded about an E-W-trending axis (stereonets d and e of Fig. 6).

7. Inter-Limb Continuity

Connectivity between the Eastern and Western Limbs has been extensively debated (e.g. Cousins, 1959; Walraven and Darracott, 1976; Cawthorn and Webb, 2001; Webb et al., 2004, 2011; Cole et al., 2013; Finn et al., 2015 and McCall, 2016). It has been proposed that limbs are discrete or separate, without connectivity at depth; that the complex is continuous; or that it is continuous but locally disrupted by domes and/or major structures. Early evidence that no RLS occurs at depth, between the limbs of the main chamber, was provided by Cousins (1959), who pointed out that there was no positive gravity anomaly in the Pienaarsrivier/Bela-Bela area, thereby implying that mafic units are not continuous at depth. Modelled gravity data was interpreted as showing intrusions with separate vertical feeders, such as those that apparently emanated from the edges of a crust-penetrating mantle diapir (see also Hatton and Schweitzer, 1995). Gravimetric studies (Kleywegt and Du Plessis, 1986; Du Plessis and Kleywegt, 1987) and geoelectric surveys (Meyer and De Beer, 1987) proposed that mafic units were probably absent between the Rooiberg Fragment and the Dennilton Dome (Fig. 6). A series of models, which center on individual, inward-dipping sheets, were presented by Molyneux and Klinkert (1978), Du Plessis and Kleywegt (1987), Meyer and De Beer (1987), Stannistreet et al. (1986) and Sharpe and Snyman (1980), who also essentially supported the idea of discrete or separate limbs. Cheney and Twist (1991) reported that geophysical data, available at the time, seemed to support the absence of RLS, at depth, in the central part of the main chamber. In terms of geometry, intrusion of a horizontal sill into a gently-folded basin constituted the model by Von Gruenewaldt (1979), while a summary in Eales et al. (1993) concluded that the complex's sheets were emplaced horizontally.

Limb connectivity or continuity at depth has been increasingly proposed in more recent studies (e.g. Cawthorn et al., 1998; Cawthorn and Webb, 2001; Webb et al., 2004, 2011). A crucial observation by Cawthorn and Webb (2001) is that there is considerable evidence for at least intermittent development of Bushveld Complex mafic units between the Western and Eastern Limbs, to the east of Pretoria. Other studies point to a substantial thickness of the complex in the center of the two limbs; Cole et al. (2013) identified areas to the west of the Wonderkop and Stofpoort Faults wherein the Upper Zone was delineated by narrow, linear, east-trending, very high amplitude anomalies and strong layering, with 70° (S) dips. To the west of this, the Upper Zone is covered by Karoo Supergroup sandstone and basalt, although magnetic data suggest that the complex continues for a further 11 km, which is coincidently the approximate width of the Marble Hall Fragment. Cole et al. (2013) stated that magnetite-rich Upper Zone rocks produce most of the observable positive magnetic anomalies and layering that outline and define the internal geometry of the Rustenburg Layered Suite across its three main limbs (*viz.* Eastern, Western and Northern). Cole et al. (2013) however, also state that magnetic data at the time was not entirely useful in the delineation of the Critical or Lower Zones due to their lack of significant magnetic minerals. Strongly remnantly-magnetized rocks in the Main Zone also contribute locally to this pattern.

The Southern African Seismic Experiment demonstrated that the crust underneath the Bushveld Complex is 44–48 km thick, compared to an average crustal thickness of 38 km for undisturbed Kaapvaal Craton. This implies an additional 6–10 km of crustal thickness in the central part of the main intrusion (e.g. Nair et al., 2006; Kgaswane et al., 2009). Cole et al. (2013) and Cole et al., 2014 also allude to unexplained gravity highs, which were attributed to up-folds of Bushveld Complex mafic units. Pre-Karoo volcanic sequences were identified by Frick and Walraven (1985) in drillcore, although basaltic or trachytic units are insufficiently dense to produce the observed Bouguer anomaly (Cole et al., 2014). Gravity profiles may be constructed such that they demonstrate continuity of mafic units in the complex's central region, provided continental crust is depressed by 6 km, thereby accounting for the 6–10 km thicker crust in this area. Nair et al. (2006), cited in Cole et al. (2014), suggested that "the smaller amplitudes may be due to less coherent stacking of events that originated from a deeper Moho." The effects of major structures and domes must also be considered in - or superimposed on - these broader models. Notwithstanding these studies, very similar mafic sequences in the Western and Eastern Limbs suggest that they formed within a single intrusion or chamber (McCall, 2016), whereas the other limbs tend to display more differences - and internal differences (Kinnaird et al., 2017) - than similarities with

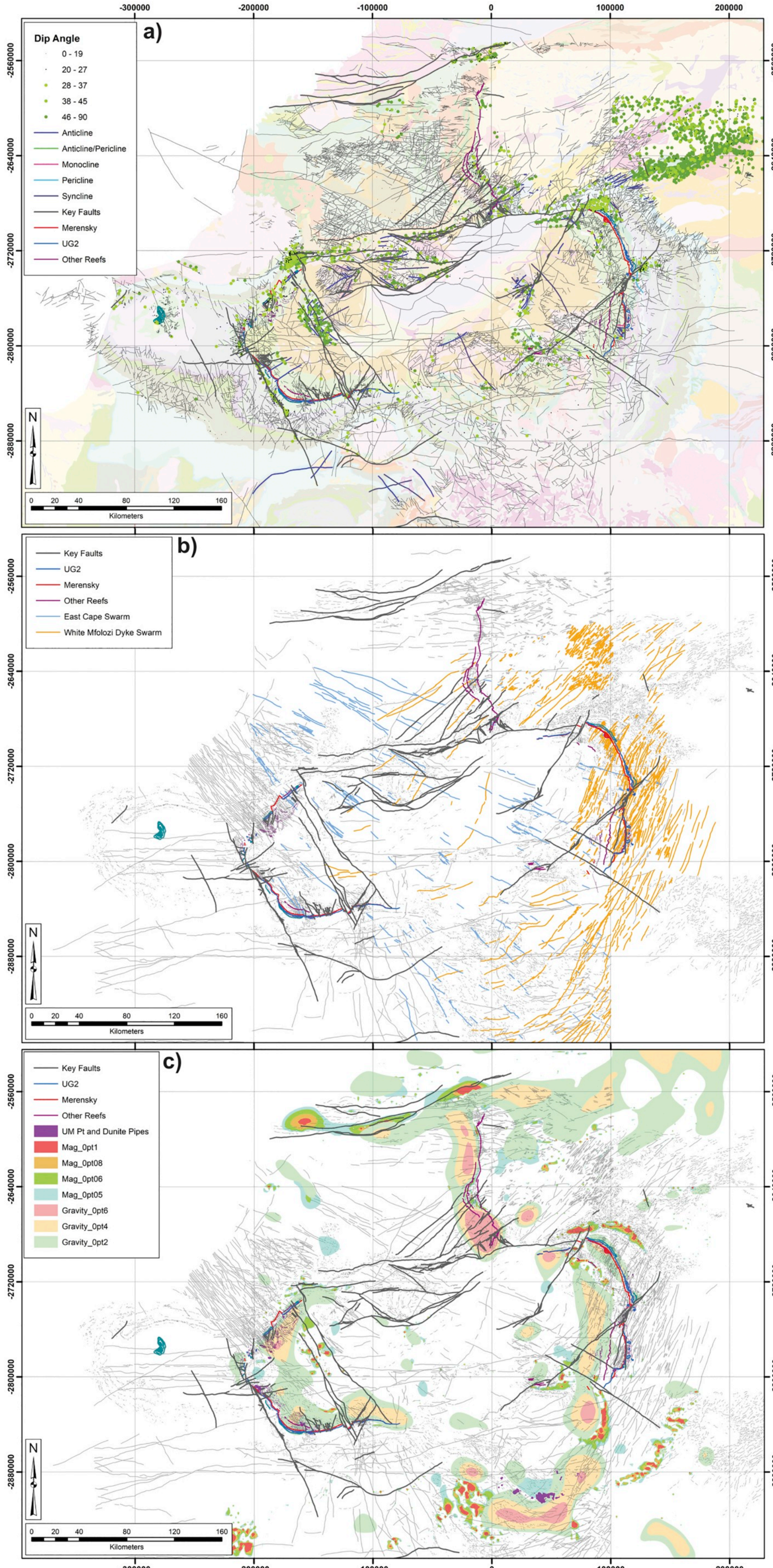

(caption on next page)

Fig. 7. Combinations of various datasets used in the final analysis: a) Background lithology (from the CGS), key faults (major structures), outcrops of main reefs (e.g. UG2, Merensky) and the distribution and dip angles of readings analysed in stereonets in Figs. 3–6; b) Key faults, outcrops of main reefs, key dykes and detailed fabric map. Pilanesberg Dyke swarm and E–W trending dykes shown in light grey; c) Key faults, reef outcrops, isoshells from gravity data inversion; isoshells from aeromagnetic data inversion. See text for details.

respect to the main chamber (Eales and Cawthorn, 1996).

Cawthorn (1998) and Cawthorn and Webb (2001) acknowledged pre-magmatic deformation in the footwall to the complex and its role in barrier or partial barrier formation, with respect to the lateral migration of magma. They also point out that the overall gently dipping, synclinal geometry of the complex is interrupted by diapiric structures at a variety of scales, following the model of Hartzer (1995) who cited thinning of the Bushveld Complex proximal to domes, rather than the RLS overlying such domes, possibly contradicting models by Uken (1999) and Gerya et al. (2003). Kinnaird and McDonald (2005) re-iterated that the Northern Limb is separated from the rest of the Bushveld Complex by the ENE–WSW trending TML, which may have comprised a dyke-like feeder for magmas, a permanent barrier or a temporary barrier between this limb and the remainder of the complex. Finn et al. (2015) modelled moderately thick, high density material near the intersection of faults within the central and western TML, which they interpreted as feeders, provided deformation in this area was relatively limited. More recent work by Kinnaird et al. (2017) proposes that - even within a single limb (namely the Northern Limb) there may be sub-chambers wherein intrusion and crystallization of the cumulate pile was distinct.

The central-northern area of the main chamber is largely obscured by sediments of the Waterberg and Karoo Supergroups (Fig. 6; Richards, 1987). Only a handful of Bushveld Complex outcrops or occurrences have been identified, including Merensky Reef on the farm Welgevonden. Upper Zone material immediately west of the Marble Hall Dome (Hartzer, 1995), and Rhenosterhoekspruit, 40 km east of Thabazimbi, where > 1200 m of layered magnetite gabbro was documented by Eales and Cawthorn (1996). Cawthorn and Webb (2001) state that the thickest development (or preservation?) of Lower Zone units occurs in the Western Limb of the complex, to the south of Thabazimbi, at Union Section and in the Olifants River Trough within the Eastern Limb. Cawthorn and Webb (2001) also state that to the east of Brits and south of Roossenekal (see also Scoon and Mitchell, 2012), Lower and Critical Zone rocks are absent, while only Main and Upper Zones are preserved. At Cullinan, the Premier diatreme transects a thinned Main Zone sequence (Bartlett, 1994), but the Upper Zone is absent (Cole et al., 2013). Portions of the upper part of the Critical Zone have been drilled nearby (Cawthorn and McKenna, 2006), while the same drillhole intersected a 260 m thick norite and pyroxenite at 530 m below surface (mbs) and the metamorphic aureole of the complex in Pretoria Group floor rocks, thereby implying that the Lower Zone is also absent. A drillhole on Fairfield Farm, near Moloto, intersected > 300 m of olivine-apatite-magnetite-bearing rocks which exhibited initial Upper Zone Sr^{87}/Sr^{86} ratios, at 587 mbs (Cole et al. (2014). The drillhole ended in the same gabbro at 917 mbs (Moen, 1989; Walraven, 1987). The Palmietgat Kimberlite, in the central part of the Bushveld Complex, yielded chromite-bearing feldspathic pyroxenite xenoliths (Webb et al., 2011), similar to the upper Critical Zone. Further southwards, Cheney and Twist (1991) designated the Dwarsfontein Complex as a thrust outlier that defined the extent of sub-outcropping Bushveld Complex. The northern and southern limbs of the Dwarsfontein Complex are bounded by E-trending faults (Pretorius et al., 1986). Significantly, despite the presence of an unconformity, mafic rocks are absent both in a 20 km gap south of the south-bounding fault and to the northwest between the complex and Pretoria (Pretorius et al., 1986). Approximately 25 km southwest of Balmoral, Martini (1998) documented a small outcrop of Upper Zone (Cole et al., 2013), which is ostensibly the western extent of the abovementioned Dwarsfontein Complex or thrust outlier. Hunter (1976) cited a galena-bearing vein, striking NW, approximately 80 km to the east of Johannesburg, which was mined until 1925. There is consequently a substantial list of intermittent exposures and intersections of mafic material, attributed to the Bushveld Complex, between its Western and Eastern Limbs. Collectively, these suggest that parts of the complex - predominantly the Upper Zone - are substantially preserved in the center of its two main limbs, although the exact geometry and depth of this central part has not been fully resolved.

8. Dykes as markers of cumulative strain

Research by Hunter and Reid (1987), Hanson et al. (2004); Letts et al. (2005), Klausen et al. (2010), Cole et al. (2013), de Kock et al. (2014), Olsson et al. (2016) and Gumsley et al. (2016), amongst others, highlights the plethora of dykes that transect the Bushveld Complex (Figs. 2, 7b and 8). Cole et al. (2013) and Greyvensteyn (2001) identified four main sets of linear, magnetic anomalies, which were interpreted as dyke sets, across the greater Bushveld Complex area:

i) NW-trending negative magnetic anomalies traverse a large part of the Western Limb and are dated at 1219 ± 6 Ma–1268 ± 10 Ma (red syenite, $^{40}Ar/^{39}Ar$ feldspar dating) and 1139 ± 18 Ma (grey syenite, $^{40}Ar/^{39}Ar$ amphibole dating) by Lee (2016). This extends from the Pilanesberg Complex, well into Botswana, and is known as the Pilanesberg Dyke Swarm/Pilanesberg Alkaline Province;

ii) A set of dykes to the NE of the Pilanesberg Dyke Swarm and to the east of the Crocodile River and Brits Graben Faults, sometimes referred to as the East Cape dyke set or swarm, but which are distinct in composition from Pilanesberg-age dykes, trend broadly NW, and exhibit a splayed geometry. Greyvensteyn (2001) labels these as "Unknown" in her compilation;

iii) NE-trending dykes, particularly to the E and SE of the study area, yield several ages, suggesting numerous phases, reactivation and emplacement along a NE trend. Significantly older dykes, in the form of the White Mfolozi Dyke Swarm (WMDS), with a weighted mean age of 2662 ± 2 Ma (Gumsley et al., 2016), albeit sampled 150–300 km to the SE of the Bushveld Complex, follow a NE trend. Klausen et al. (2010), in the Black Hills area immediately to the east of the Eastern Limb, cite ~1.90 Ga NE-trending dykes which show a similar geochemistry to ~1.93–1.87 Ga post-Waterberg dolerites studied by Hanson et al. (2004). Furthermore, positive linear anomalies parallel to the Olifants River Dyke Swarm (ORDS; Uken and Watkeys, 1997b), were interpreted as being distinct from Karoo-aged dykes (~182 Ma);

iv) Extensive East-West trending dykes, characterized by positive magnetic linear features, which transect the entire Bushveld Complex. Baddeleyite U–Pb analyses, from six short dolerite dykes to the east of the Bushveld Complex, yield dates in the 2.685–2.660 Ga age-range. However, these are not continuous with, and cannot be traced into, newly-interpreted dykes that show no signs of bending and which suggest their late, possibly Gondwana-break up, emplacement.

According to Uken and Watkeys (1997b), Burke and Dewey (1973) sited a triple-point junction and the Karoo plume position on the Nuanetsi Igneous Province. This locality corresponds to the junction of the Okovango Dyke Swarm and the WMDS. For ease of reference, the NE trend is referred to as the WMDS trend throughout this contribution, although the reader should bear in mind that the Black Hills dykes and the WMDS follow the same trend. Examination of the WMDS reveals

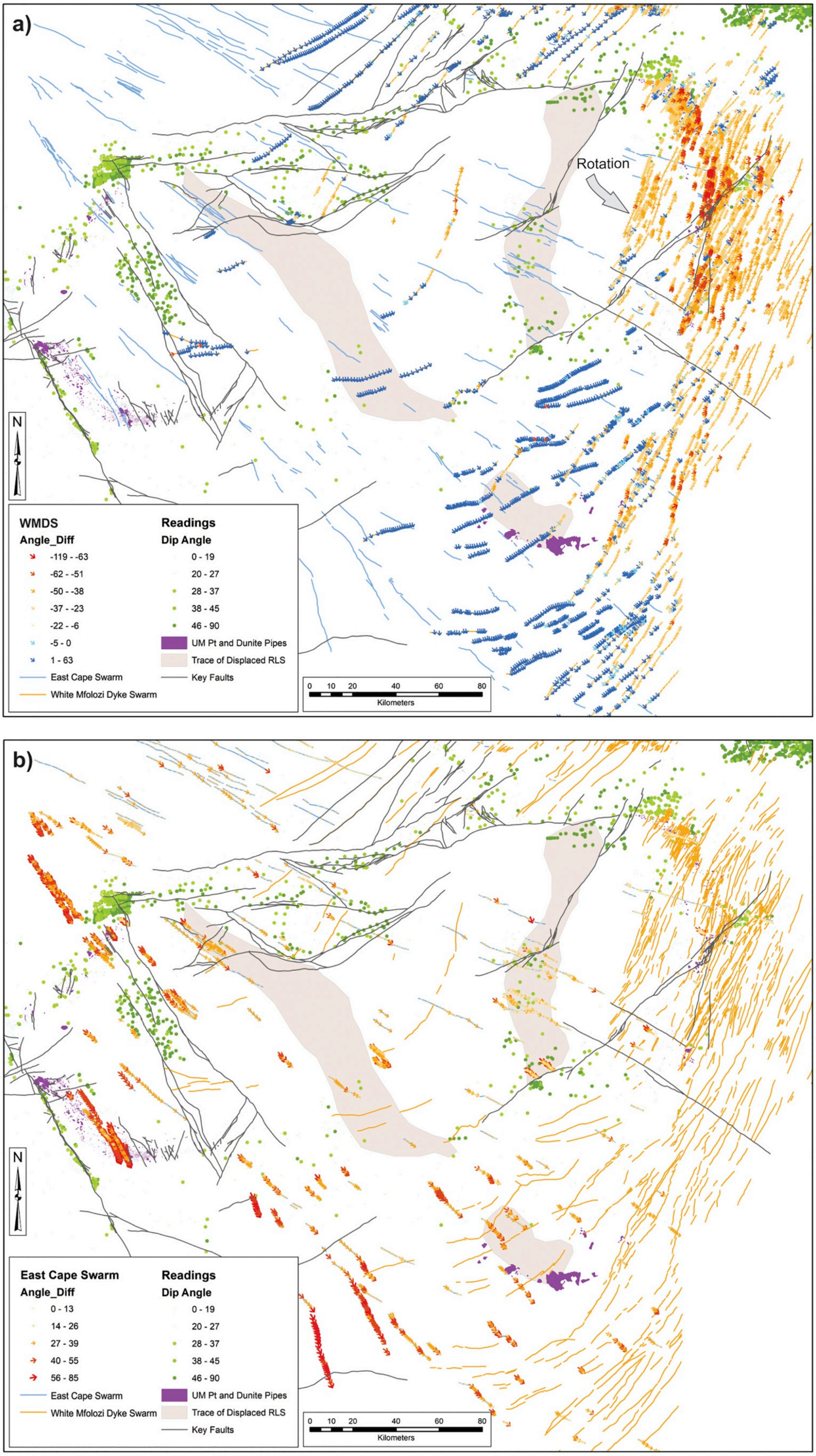

Fig. 8. Analysis of dykes as proxies for strain (using older dykes as "strain markers"). The White Mfolozi Dyke Swarm (WMDS), highlighted in a), shows progressive anticlockwise rotation relative to the initial 054° trend of its NE portions. Splaying of these dykes is progressively greater from NE to SW, with increasing distance from the "inflection point" or "inflection line" in the vicinity of Gravelotte. The red arrows on a) denote this broadly NNW-trending zone of significant rotation and thereby high angular strain. Orientations change as dykes are rotated clockwise around the apex of the thrust-displaced RLS. The East Cape Dyke swarm highlighted in b) also shows progressive splaying or separation between dykes, from NW to SE and relative to an initial orientation of 100°, although this is less obvious than that of the WMDS, due to the acute angle of this swarm to the inferred displacement vector to the SSE. Maximum cumulative deformation occurs over the central part of the Southern Limb, 335 km SSE of the TML. The occurrence of a large body of IRUP near this apex and just to the SE of a thrust-displaced fragment of high-density material suggests significant Fe-rich fluid expulsion from the deeper parts of the complex.

that there is an inflection in its trend (Figs. 7b and 8) in the vicinity of Gravelotte. North of the inflection point, dykes trend 054°, while to the south of the inflection point, the same dykes are rotated anticlockwise, to approximately 020°. Post-emplacement movement along these NNE-trending dykes was determined by Uken and Watkeys (1997b), who pointed out that while the broadly NE-trending WMDS follows the main axes of the 2.7 Ga Ventersdorp rift system, as defined by Stannistreet and McCarthy (1991), dykes have amphibolite-bearing margins caused by left-lateral, strike-slip movement that post-dates the 2.0 Ga Phalaborwa Complex syenite. Uken and Watkeys (1997b) also noted that there are two ages and compositions of dykes: diabase dykes or altered mafic dykes in the north (see Schwellnus et al., 1962) and dolerites or unaltered mafic dykes in the south. Karoo-aged dolerite dykes locally transect diabase dykes but generally re-utilize the dominant, earlier trend in the granitoid basement. Uken and Watkeys (1997b) concluded by stating that “The twisted, southern part of the WMDS, south of the inflection point, was re-utilized during the Karoo, guided the trend of the Drakensberg escarpment and Gondwana breakup”. Consequently, older diabase dykes have rotated anticlockwise, to the SW of the abovementioned inflection point and across the greater part of the main Bushveld Complex chamber. Fig. 8a shows that these dykes are “splayed” or exhibit progressively greater inter-dyke spacing from NE to SW, particularly across the center of the main chamber and the Southern Limb. Around the southern part of the main chamber and in the Southern Limb, at the southern apex of deformation, these dykes are curved, convex-south (Fig. 8a). Dykes also become more dismembered, exhibiting progressively shorter strike lengths from NE to SW. This angular shear may be visualized by plotting dyke segment-vertical scaled arrows, relative to an initial trend (in the NE) of 054° (Fig. 8a).

The set of dykes to the northeast of the Pilanesberg Complex and Pilanesberg Dyke Swarm, but to the east of the Crocodile River and Brits Graben Faults (East Cape Dyke Swarm), also transects the central part of the Bushveld Complex (Fig. 8b). These dykes show notably greater strike continuity in the north, particularly to the north of the TML, but become notably more discontinuous to the south. There is also a change in dyke trend (as for the WMDS), but in this case from approximately 100° in the north to approximately 135° in the south, concomitant with a splaying or increase in dyke-to-dyke distance towards the SSE and through the Southern Limb. This effect is more subtle, compared to the WMDS, but the pattern may also be visualized by plotting dyke segment-vertical scaled arrows, relative to an initial angle (in the NW) of 100°. Based on Fig. 7a and b, the extent of cumulative SSE-wards displacement, with respect to the TML in the north, is approximately 335 km.

Fig. 7a shows recorded dips, colored according to dip angle. It is apparent that the Murchison area, to the east of the inflection point at Gravelotte, shows a high concentration of significantly steeper dips, compared to areas along-strike and to the west, wherein strain has been dissipated through the central portion of the main chamber.

9. 3D geophysical data inversion

Cole et al. (2014) cite numerous examples wherein gravity modelling has been used to delineate the geometry of layered mafic intrusions; to these references Armit et al. (2010), Williams et al. (2016) and Rezaiea et al. (2017) may be added. The upper Pretoria Group, with a density of approximately 2720 kg/m^3, essentially hosts the RLS, in turn overlain by Rooiberg Granites with a density of approximately 2630 kg/m^3 (Coomber, 2008; Cole et al., 2014). Coomber (2008) proposes a range of 2595 kg/m^3 to 2630 kg/m^3 and a value of 2620 kg/m^3 for the Transvaal Supergroup. The younger Lebowa and Rashoop Granite Suites, also with an approximate density of 2630 kg/m^3, intruded into the upper part of the RLS, thereby cross-cutting Rooiberg Felsites (Eriksson et al., 1995; Van Tongeren and Mathez, 2009; Van Tongeren et al., 2010). Jones (2015), citing Cawthorn and Spies (2003), Ashwal et al. (2005a, 2005b) and Davis et al. (2007) and summarizing density measurements from available drillholes and mine workings, lists undifferentiated granitic units as having a density of 2660 ± 60 kg/m^3. Coomber (2008) proposes a range for “heterogeneous Bushveld Complex” of 2870 kg/m^3 to 2980 kg/m^3. In terms of average or typical values for individual RLS units (Cole et al., 2014; Jones, 2015), the following are reasonable: Marginal Zone: 3054 kg/m^3; Lower Zone: 3196 kg/m^3; Critical Zone: 3090 kg/m^3; Main Zone, 2920 kg/m^3; Upper Zone: 3110 kg/m^3 and an average value for iron-rich ultramafic pegmatoids of 3091 kg/m^3 (Coomber, 2008). Consequently, there is a notable density contrast between host sedimentary units, the main part of the Bushveld Complex (the RLS) and granites. Regional geophysical maps show prominent gravity highs associated with well-constrained or mapped limbs of the complex (e.g. see Fig. 3 of Cawthorn and Webb, 2001 and Fig. 2 of Webb et al., 2004). Regional gravity data used in this study are available as a gravity database, for the whole of South Africa, from the Council for Geoscience (Council for Geoscience, 1997) and includes 19214 data points within the Bushveld Complex (see Coomber, 2008 and Cole et al., 2014).

Hattingh (1991), Ferré et al. (1999) and Ashwal et al. (2005b) summarize the magnetic susceptibility of the RLS, while Campbell (2011) discusses the modelling of magnetic data across the complex. There is a broad range of susceptibilities due to the intricate cumulate layering of the Bushveld Complex and a plethora of thin magnetite and chromite stringers and reefs. Hemant (2003) summarizes magnetic susceptibilities for typical rock types and packages: gabbro 0.09 SI units, norite 0.09 SI units, pyroxenite/hornblendite 0.25 SI units, dunite 0.125 SI units and “Avg. Basic igneous rock (komatiites, tholeiites)” at 0.12 SI units. Hemant (2003) also lists Transvaal Supergroup as 0.034 to 0.092 SI units. Magnetic susceptibility data highlight the Main Zone-Upper Zone boundary, while Main Zone cumulates almost invariably have magnetic susceptibilities < 0.05 SI units, and commonly as low as < 0.02 SI units (Hemant, 2003). The same study also cites < 1 to 5 m granitic sills in the Main Zone, showing a response of up to 0.7 SI units. There is more variability in magnetic susceptibility above the Main Zone:Upper Zone Boundary, with anorthositic layers at values below 0.1 SI units and magnetites up to 5 SI units. The open-source, SA's Council for Geoscience, 3 km line-spaced regional airborne magnetic dataset was used in potential-field inversion modelling (see Ledwaba et al., 2009).

3D, unconstrained forward models of inverted density and magnetic data produce models (e.g. Tchikaya et al., 2016) that are geologically-plausible and accord with observed gravity or magnetic susceptibility anomalies. The most useful outputs are voxels (or voxets), of relatively high density and magnetic susceptibility, extracted from unconstrained inversion volumes. These essentially reflect a percentage difference with respect to a background value and are the products of a numerical procedure that fills the interior of a subsurface mesh with physical property values, derived from measured magnetic or gravity data, within a specified error tolerance and/or deviation from a background value (Li and Oldenburg, 1996, 1998; Fullagar and Pears, 2007), in this case values within the Pretoria Group. It should be noted that unconstrained inversions produce only one of several possible physical property models, all of which are consistent with both data and observations. In this study, models were created using Paradigm GoCad and inverted using Fullagar's VPmg software. Gravity data were inverted in two steps, commencing with a basement inversion, followed by a heterogeneous density inversion. Fig. 7c shows Bouguer-corrected density relative to a background of 2670 kg/m^3. The resolution for the gravity model, in terms of cell size of the voxet, is 2000 m horizontal × 100 m vertical. Also shown on Figs. 7c and 9 is the result of a two-step magnetic data inversion, comprising an initial basement inversion to remove the regional field, followed by a heterogeneous susceptibility inversion. The starting background susceptibility in the first step was set at 0, with the resulting model seeded into the subsequent heterogenous inversion stage/model with the half-space value maintained at 0. The resolution of magnetic susceptibility voxets is

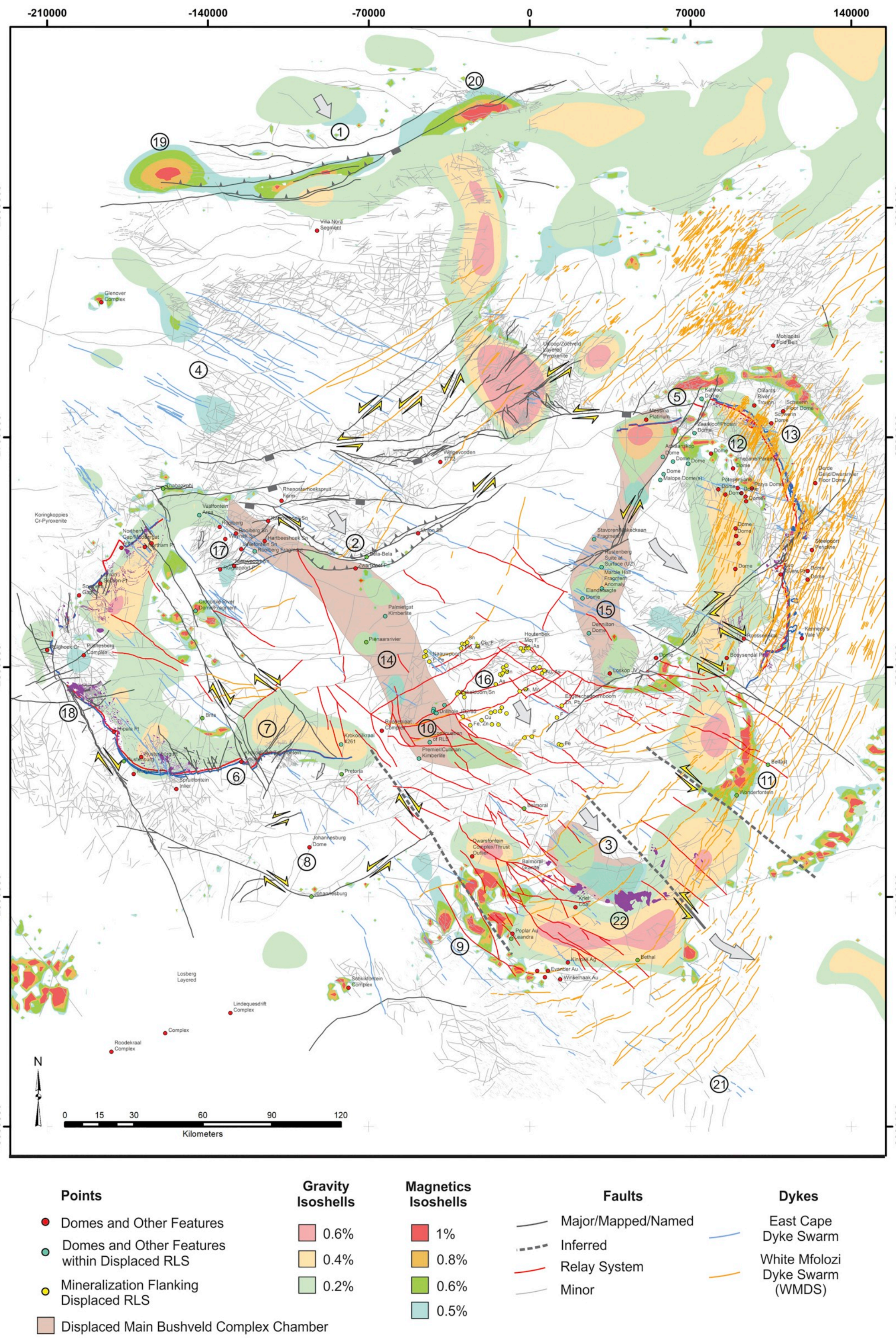

Fig. 9. Summary of features, including: kinematics of major structures; distribution of gravity and magnetic isoshells; rotation and splaying of the WMDS and East Cape Dyke Swarm; the combined distribution of domal features and anomalous occurrences of Bushveld Complex throughout its central part; rotation of the Burgersfort Bulge (originally an E-directed lateral tectonic escape structure); a suite of brittle to brittle-ductile relay structures (in red), which accommodated southward movement and the interpreted trace or extent of the dismembered northern margin of the main chamber of the Bushveld Complex. The extent of this southward movement may be strongly delimited or affected by the Steelpoort-Klopperskloof-Rietfontein Fault(s). It is proposed that the western extent of the Southern Limb was also connected to the eastern extent of the Western Limb, but was displaced by a combination of right-lateral brittle to brittle-ductile faults (the Crocodile River and the Brits Graben/Hartebeespoort Faults) and the competency contrast around the northern margin of the Johannesburg Dome, in concert with a set of ductile, right-lateral shears at depth and further south. This movement may have been responsible for post-Bushveld expulsion of fluids to form the HITIS, features of the Transvaalide Fold-and-Thrust event and NNW-trending magnetic isoshells around the Dwarsfontein Complex or outlier. The proposed trace of the dismembered and displaced main chamber of the Bushveld Complex is shown as a brown polygon. The following discussion addresses particular points of interest (1 – 22).

2000 m horizontal × 500 m vertical.

Fig. 9 shows density and magnetic susceptibility isoshells, combined with major faults, fabrics and key points mentioned in a previous section on the continuity of the Bushveld Complex. Several patterns are immediately noticeable. To the north of the TML, the eastern part of the Northern Limb, the Villa Nora Complex (bounded by the Abbotspoort Fault Zone) and the Glenover Complex are defined by both density and magnetic susceptibility isoshells. Notably, Fig. 9 shows only scattered or minor occurrences of dense material over the western portion of the Northern Limb, between the Glenover Complex and the Thabazimbi area, suggesting that much of the Northern Limb is either poorly-developed or missing. The Western Limb to the south of the Thabazimbi area shows two southward inflections or bends: in the Vaalfontein Area and the Krokodilkraal 4261 area to the north of Pretoria; both instances occur to the east of the Crocodile River Fault. Further southwards, there is a gap of 50–70 km between density anomalies that define the eastern extent of the Western Limb and the start of the Southern Limb. Significantly, this gap is very similar to the proposed horizontal offset due to southward-verging thrusts or transposed normal faults (Droogekloof Thrust, Boschpoort Fault/Thrust and Southern Boundary Fault to the south of Thabazimbi) which, as noted elsewhere in this contribution, mimics the southward-verging geometry and curvature of the Abbotspoort Fault Zone in the northern part of the Northern Limb (Villa Nora area).

The patterns in the central part of the complex are also instructive. A collection of "points of interest", including the anomalous occurrences of Bushveld listed previously, several negative magnetic anomalies (shown on the geophysical inversion map), drillholes FF1/85, VF1/85, JD1/85 and JD2/85 and the Moloto/Fairfield area (Walraven, 1987), several Cu (Fe and Zn) occurrences, Bushveld Complex intersections at the Premier/Cullinan Diamond Mine, Argent Mine and gravity isoshells collectively define a NNW trend (Fig. 9). Towards the Eastern Limb, a N–S to NNE trend is defined by a combination of denser areas and the Dennilton Dome (Hardwick et al., 2015), the Elandslaagte Dome (Hartzer, 1995), the Marble Hall Fragment Anomaly (e.g. Babayeju, 1999), occurrences of possible Upper Zone at surface and the Kwagganek structure (Hartzer, 1995), the Stavoren/Makeckaan Fragment (Schweitzer et al., 1997), the Malope Dome(s) (Johnson et al., 2004) and the Zaaikloof/Phosiri Dome (Schweitzer et al., 1997). Another point of interest is that there is a high density of F, Fe, Zn, Pb, Cu, Co, Mo, Ni, Ag, Au, As, Th and REE occurrences to the north of and skirting the inner margins of these two trends (Fig. 9). Magnetic susceptibility isoshells show a symmetry with respect to the Southern Limb (Fig. 9). The "deep-seated, remnantly-magnetized body" of Cole et al. (2013), in the east, has an analogue or "twin" on the western end of the Southern Limb; however, the easternmost body shows two sets of curvilinear trends, while the westernmost body, overlapping with the Dwarsfontein Complex or Thrust Outlier, shows a series of NW- to NNW-trending linear trends that are along-strike with the Crocodile River Fault to the north.

10. Syn- to post-Bushveld deformation, Transvaalide Fold-and-Thrust event and HITIS

There is a body of work and radiometric dating that record a series of younger ages or events, over approximately 5–10 Myr, following emplacement and the rapid cooling of the bulk of the complex. Nomade et al. (2004) extracted integrated and plateau ages of 2037 Ma to 2049 Ma, with a weighted mean age of 2042.4 ± 3.2 Ma, from biotite at Impala Platinum Mine (Fig. 4). The authors noted low-angle thrusting and biotite formation from circulating fluids (see also Robb et al., 2000), in line with pervasive alteration and overprinting of the Critical Zone during "post-crystallization, syn-cooling, hydrothermal circulation" (e.g. Schiffries and Rye, 1990; Schiffries and Skinner, 1987 and Merkle, 1992). An overlapping age is provided, by Re-Os isochron dating, of 2043 ± 11 Ma (Schoenberg et al., 1999) on similar material.

Following work by Parsons and Killick (1990), Hilliard and McCourt (1995), Bumby et al. (1998), Gibson et al. (1999) amongst others, Alexandre et al. (2006) examined the Transvaal Supergroup between the Bushveld Complex and the Vredefort Structure, i.e. to the south of the area studied by Nomade et al. (2004). The area experienced regional, low-grade metamorphism, synchronous with brittle-ductile deformation, small- to meso-scale folding, cleavage formation, and the development of monoclines and thrusts in dolomite, slate and phyllite. Alexandre et al. (2006) undertook single-grain, $^{40}Ar/^{39}Ar$, step-heating, laser probe dating of syn-kinematic white mica from phyllite, producing ages of approximately 2150 Ma and 2042.1 ± 2.9 Ma (plateaus and pseudo-plateaus, respectively). These were considered distinct from both the emplacement age of the Bushveld Complex and the age of the Vredefort Structure (~2.02 Ga). Scoates and Friedman (2008) determined that the Upper Platreef and the Merensky unit are statistically contemporaneous in terms of their U-Pb zircon ages, but that younger zircon ages in chromitites from deeper, more "chemically primitive" units imply that late-magmatic, high-temperature processes were active over a period of > 10 Ma, post-emplacement of the complex. These observations, combined with shallowly north-dipping thrusts and recumbent folds verging eastwards and southwestwards, reflect conclusions by Andreoli (1988b): Transvaal Supergroup units, and possibly the deeper portions of the complex itself, were subject to the "Transvaalide fold-and-thrust belt" at or after approximately 2.04 Ga, although this event was originally related to orogenic activity along the (northern?) margin of the Kaapvaal Craton, as per Kamber et al. (1995) and Holzer et al. (1998).

In summary, Alexandre et al. (2006) and Andreoli (1988a, 1988b) suggested a succession of ages/events overlapping with to immediately after the intrusion of the Bushveld Complex. Firstly, 2123.4 ± 22.5 Ma fabrics in Transvaal Supergroup phyllites immediately west of the Rustenburg Fault (Figs. 4 and 8; refer to Table 3 in Alexandre et al., 2006), accord with regional, pre-BIC tectonic activity near Rustenburg and in the floor of the complex to the west of Pretoria (Bumby et al., 1998; Hartzer, 1995). This "~2.15 Ga event" was linked to pre-Bushveld folding and thrusting, described by Bumby et al. (1998). Secondly, the well-constrained 2.06 Ga emplacement of the Bushveld Complex, its associated thermal metamorphism, the formation of hornfelses and extremely rapid cooling ensued (e.g. Zeh et al., 2015). This was followed by the development of a series of fabrics/phyllites at 2042.1 ± 2.9 Ma, to the east of the Rustenburg Fault (Alexandre et al., 2006; Figs. 4 and 8). Andreoli (1988a, 1988b) suggested that this ~2.04 Ga age implied complete resetting of older, Bushveld Complex-age micas during a post-Bushveld tectono-thermal event involving folding and thrusting, focused in or along the least competent stratigraphic units within the study area, while Scoates and Friedman (2008) alluded to the same effects in the hotter, deeper parts of the complex. The Uitkomst Complex, which is a Ni-Cu-PGE-Cr-mineralized layered basic intrusion 200 km due east of Pretoria, shows a concordant $^{207}Pb/^{206}Pb$ zircon age of 2044 ± 8 Ma, which De Waal et al. (2001) suggested was broadly "coeval" with the RLS. While Andreoli (1988b) related this event to a ~2.05 to ~1.98 Ga transpressive-compressive orogenesis and high-T metamorphism in the Central Zone of the Limpopo Belt, concomitant with the reactivation of the Palala Shear Zone, it is worth reiterating that Alexandre et al. (2006) concluded that the 2042.1 ± 2.9 Ma phyllite age is distinct from both the Bushveld Complex intrusion and the effects of the Vredefort impact event. These authors also state that these ages denote "a separate, dynamothermal episode of mica growth under tectonic conditions favourable for the development of regionally extensive cleavages". These events were, in turn, followed by the *c.* 2.02 Ga Vredefort impact structure (e.g. Kamo et al., 1996).

There are numerous, layer-parallel structures, including thrusts and synthetic shears recorded at Marikana Platinum, Rustenburg Platinum, Booysendal Platinum, the Premier/Cullinan Diamond Mine and elsewhere throughout the complex (e.g. Viljoen and Hieber, 1986; Treloar and Steenkamp, 2000; Perritt and Roberts, 2007; Roberts and Clark-Mostert, 2010; Couto and Theron, 2014; McKechnie et al., 2015; Qamata and Steenkamp, 2016), primarily from geotechnical or geological engineering studies on mines in the southern part of the Western Limb. Faulting parallel to the primary Bushveld Complex layering is generalized as "shallow roof discontinuities" or "dome structures" parallel to the cumulate layering, although descriptions and pictures suggest south-verging thrusts. According to McKechnie et al. (2015), on Sibanye Gold's Rustenburg operations on the southwestern part of the Western Limb, very low angle faulting is focused at the base of the Boulder Bed and the top or base of the Footwall Marker. The Footwall Marker, 12 m below the Merensky Reef, has been transformed into a thrust with variable displacement (mm to > 12 m) and shows fault gouge from a few mm to approximately 5 cm wide. Clarke et al. (2000) analyzed the Spruitfontein inlier and the surrounding RLS. They resolved several key deformation events: D_1 caused by NNW-SSE-directed compression, accompanied by the formation of ductile structures and upright to steeply-inclined, shallowly ENE-plunging cuspate folds with sub-vertical, ENE-trending planar foliations. This was followed by a brittle D_2 event, which formed a "prominent, sub-vertical conjugate hybrid extension shear-joint system". Joint (and fault) sets strike NNW and ENE. Overall, associated steep, southward-verging reverse faults and proximal isoclinal folding attest to the broader pattern of S-directed thrusting.

The area east of the Rustenburg Fault, north of the Johannesburg Dome and to the west of the Southern Limb of the Complex is also occupied by a relatively late, high-Ti igneous suite (or the HITIS). These are km-scale mafic igneous bodies that are concentrated on and around the northern rim of the Vredefort structure and significantly east of Pretoria, to Heidelberg (see references in De Waal et al., 2006 and Ernst, 2014). Such bodies include the Roodekraal Complex, the Lindequesdrift Intrusion, the Rietfontein Complex and the Kaffirskraal/Schkikfontein Complex. HITIS are characterized by: augitic to salitic clinopyroxene, plagioclase (An < 50), magnetite (± ilmenite) and late-magmatic amphibole (edenite-magnesiohastingsite) (De Waal, unpublished information, cited in De Waal et al., 2006) and general enrichment in Cu (Cu/Ni ratio ~ 12.5). In the case of the Roodekraal Complex, small Cu segregations occur along faults and contact zones (Clark, 1972, cited in De Waal et al., 2006) and zoned, hydrothermally-overprinted ore bodies, ranging from magmatic high-temperature chalcopyrite-pyrrhotite-pyrite assemblages, through chalcopyrite-chalcocite, to low temperature chalcocite-bornite assemblages (De Waal et al., 2006) are common. These authors conclude that geochemical data shows that the Roodekraal Complex was produced by fractionated, residual liquid or magma extruded or expelled from a more mafic, deep-seated, precursor magma within a fractionating system, genetically-related to the Lindequesdrift and Heidelberg Intrusions. Further eastwards and directly along strike with the Laersdrift Fault (Fig. 3), the Uitkomst Deposit/Complex (concordant $^{207}Pb/^{206}Pb$ zircon age of 2044 ± 8 Ma (Gauert et al., 1995, 1996; Gauert, 1998, 2001 and De Waal et al., 2001) comprises a Ni-Cu-PGE-Cr-mineralized layered basic intrusion with commercial levels of magmatic base-metal sulfides. De Waal et al. (2001) recognized boninitic Bushveld magmas as being parental to both the lower ultrabasic and upper basic layered series of the complex, with its textures suggestive of magma mixing and contamination. Gauert et al. (1995) furthermore presented evidence of post-intrusion, steeply-dipping faults that are perpendicular to the NNW strike of the body. These resulted in N-upwards, vertical displacement (i.e. reverse faulting with a southward vergence) of tens of meters. Hornsey (1999), cited in Joubert et al. (2006) observed that the complex underwent post-emplacement, diabase sill intrusion and layer-parallel thrusting. As the Lindequesdrift Complex is cross-cut by a 2023 ± 4 Ma pseudotachylite generated by the Vredefort structure or event (Kamo et al., 1996), which is "a feature common to all the HITIS rocks in the Vredefort area" it is clear that the majority of HITIS bodies also pre-date the Vredefort event.

There is also evidence of syn-RLS-crystallization faulting (Clarke et al., 2005; Gauert et al., 2013) in the eastern part of the complex. Clarke et al. (2005) documented syn-Bushveld folding of the RLS adjacent to the Steelpoort Pericline, near the Steelpoort Fault. As the Steelpoort Fault, which transects the Eastern Limb, is approached from a southerly direction, the density and/or size of iron-rich pegmatoids, split reefs and potholes increase dramatically, PGE grades decrease (e.g. at Two Rivers Platinum Mine) or are erratic (e.g. Kennedy's Vale/Rhodium Reefs Mine), and general disruption of the magmatic or cumulate layering becomes more prevalent (Gauert et al., 2013). The latter authors concluded that post-intrusion faulting provided a magma conduit that was exploited by late-stage iron-rich liquids.

11. Discussion

There is a coherent pattern of syn- to post-intrusion deformation across the Bushveld Complex (Fig. 9), which may be synthesized into a new model that also provides insight into the complex's original geometry. In the northern part of the Northern Limb, the convex-south Abbotspoort Fault Zone shows at least 50 km of southward vergence (Point 1 on Fig. 9), reflected by extensive, numerous left-lateral faults or shears, such as the Rooisloot/Mahopane, Ditlokeng, Sandsloot, Sinonela and Transcurrent/Pruizen Faults (Fig. 5). Southward vergence, of at least 70 km (Point 2) is also evident from the Droogekloof Thrust, Boschpoort Fault/Thrust and Southern Boundary Fault near the Thabazimbi/Rooiberg area. The effects of southward-verging deformation persist for approximately 170 km to the SSE of this (Point 3). Significantly, the western part of the Northern Limb is largely missing or poorly preserved (Point 4), relative to the eastern part of the Northern Limb, suggesting that the estimated 10 km N-up vertical offset cited by Good and De Wit (1997) has resulted in severe uplift and erosion of this part of the complex. The Eastern Limb is highly faulted in its northern portion (Point 5) which, along with the Mohlapitsi Fold-and-Thrust Belt and the left-lateral Wonderkop-Stofpoort Fault system, suggests predominantly N–S or NNW–SSE-directed principal stresses. Significantly steeper bedding and cumulate layering along the northern edge of the Eastern Limb, the "concatenated" or "ptygmatically-folded" eastern part of the Northern Limb and the development of a strong planar fabric (Uken, 1999) also attest to a high cumulative strain.

Southward tectonic vergence persists into the southern portion of the Western Limb (vicinity of Point 6), in the form of numerous low-angle, bedding- or cumulate-layer parallel shears in underground platinum mines, the mode of deformation in the Spruitfontein Inlier (see Clarke et al., 2000), bending and steepening of bedding and cumulate layering around the Johannesburg Dome (see Gibson et al., 1999), folding and left-lateral shearing just to the west of Rustenburg, for example along the Jukskei River Shear zone and within the Spruitfontein Inlier (Clarke et al., 2000), low angle (J4) shears at the Premier/Cullinan Diamond Mine and the development of NE-SW trending left-lateral faults such as the Schietfontein, Zilikaatsnek and Lindwe Faults (Point 7), which are effectively a result of a southward-moving complex impinging onto and around the Johannesburg Dome (Point 8). This is proposed as a stress-riser that initiated and aided the creation of an apparently separate Southern Limb.

The Crocodile River Fault terminates just to the north of Pretoria. However, a series of parallel, NNW-trending magnetic susceptibility isoshells (Point 9) occur approximately 65–70 km south of this, near the Dwarsfontein Complex/Thrust Outlier (Fig. 6), which may be attributed to significant Fe-rich fluid expulsion and movement along NNW-SSE-trending structures (see also Hayes et al., 2017b). As there is no clearly-defined fault or fault system connecting the eastern termination of the Western Limb with the western termination of the Southern Limb, and in light of the southward bend of the complex in the Krokodilkraal 4261 area, it is proposed that right-lateral offset of the southern limb from its parent body was ductile at depth but accommodated by a near-surface brittle or brittle-ductile relay system (shown in red Fig. 9, in the vicinity of Point 10). Another intriguing pattern emerges from the map of magnetic susceptibility isoshells: there is a similar cluster of highly-susceptible bodies to the north of Wonderfontein (Point 11) that is symmetrically arranged around the displaced, anticlockwise-rotated Southern Limb.

The Burgersfort Bulge (Point 12), bound on its southern margin by the right-lateral Steelpoort/Dwarsrivier Fault System and on its northern margin by the left-lateral Wonderkop Fault system, was an E or ENE-directed lateral escape structure that developed during initial compression, causing near-field E-directed stresses within the Phalaborwa Complex (Basson et al., 2017) and east-verging thrusting at numerous gold deposits to the east of the Eastern Limb. Lateral movement, within the Western Limb, was constrained to a series of strike-extensive transverse faults that were re-utilized to form syn-intrusion gap areas and grabens, but only in areas to the west of the Crocodile River Fault. Based on the anticlockwise rotation, splaying and left-lateral shearing of the White Mfolozi Dyke Swarm to the south of its inflection point (Fig. 8 and Point 13 on Fig. 9), this escape structure and the central portions of the main chamber have rotated anticlockwise by an estimated 35°, accommodated by extensive, brittle to brittle-ductile, right-lateral movement along the Crocodile River and Brits Graben Faults and was accompanied by southward thrusting of the main chamber's deeper, more ductile center. Several structures, highlighted in red on Fig. 9 (vicinity of Point 10), are interpreted as a collection of brittle or brittle-ductile relay structures that accommodated this rotation within the upper levels of the complex.

A convex-south, arcuate string of anomalous occurrences or intersections of Bushveld Complex units, combined with the distribution of domes, fragments and a series of gravity anomaly isoshells, outline the displaced northern margin of the main chamber (Points 14 and 15), probably with a macroscale dismembered or boudinaged geometry. This raises the intriguing possibility that domes may have been rotated - or formed - under a consistently-directed far-field stress, which does not negate observations and models that cite dome ductility or heat-induced accentuation of initial asperities in the floor of the complex, as these processes may have worked in concert with rotation. Signs of ductile deformation of this part of the complex may be gleaned from the southward-“dragged” or bent portions of the eastern ends of the Western Limb, highlighted by gravity isoshells, in the Vaalfontein and Krokodilkraal 4621 areas (Fig. 9). The northern or inner edge of this displaced northern margin shows a high density of F, Fe, Zn, Pb, Cu, Co, Mo, Ni, Ag, Au, As, Th and REE occurrences (vicinity of Point 16), similar in nature and host rocks to those around Rooiberg to the north (vicinity of Point 17). The southern limit of the main parts of the displaced northern margin of the chamber and displaced F, Fe, Zn, Pb, Cu, Co, Mo, Ni, Ag, Au, As, Th and REE occurrences, coincides with the SW extent of the Klopperskloof-Dwarsrivier-Steelpoort Fault system, which is almost directly in line with the Rietfontein Fault that runs through Johannesburg (Fig. 6). Although these faults are not obviously contiguous, based on available data, they appear to define a fundamental structural boundary, possibly in the form of a major, re-activated normal fault.

Several features suggest that the positions of domes and alkali intrusions were controlled by the complex's deformation. For instance, the markedly increased fracturing and density of IRUPs to the south of the Pilanesberg Complex (Point 18) attest to its southward impingement into the RLS in the Styldrift/Wesizwe/Bakubung area. De Waal et al. (2006) attributed the Lindeques Drift, Heidelberg and Roodekraal Complex (HITIS) intrusive bodies to an incipient, failed or flanking continental rift, and a single magmatic event coeval with Bushveld Complex emplacement further to the north. Their low-Al, high-Fe ferrobasaltic magma was attributed to deep-crustal amphibole-plagioclase fractionation of an alkali basaltic precursor in an embryonic continental rift setting. The distribution of magnetic susceptibility isoshells on the southern and southeastern margins of displaced components of the complex (Points 9 and 11), fabric overprints and biotite regrowths (e.g. Andreoli, 1988a, 1988b), the Transvaalide Fold-and-Thrust event, the age and location of HITIS, pervasive IRUPs and related bodies collectively denote significant, late-intrusion, stress-induced differentiation and expulsion of fluids from the deeper, less well-crystalized parts of the intrusive mass, as alluded to by Hayes et al. (2017b), concomitant with extensive southward movement of its central part and offset its southern margin, forming what is now known as the Southern Limb. The southern extent of the effects of this deformation are estimated as extending to 335 km SSE of the TML (Point 21). A large body of recorded IRUP (Point 22) occurs just to the north of a high-density fragment, suggesting a significant SE-wards movement of Fe-rich fluids around the apex of the displaced RLS. It is intriguing to note that Fig. 9 also shows two magnetic susceptibility highs/isoshells, symmetrically disposed with respect to the northern margin of the northern limb of the complex (Points 19 and 20), in an almost identical configuration to those at Points 9 and 11.

This model also accounts for en-echelon sub-basins or depressions containing the Irrigasie, Clarens and Letaba Formations of the Karoo Supergroup (Figs. 1 and 2), which ultimately occupied local pull-apart basins formed by the progressive anticlockwise rotation of the Eastern Limb and central parts of the complex. The new model presented herein may also assist in resolving the geometry and continuity of the central part of the main chamber of the Bushveld Complex, using constrained gravity inversion and modelling. For instance, severe southwards displacement of the central part of the complex, extension and dismemberment of the northern margin of the main chamber and internal thrust-duplication of the RLS could have produced smaller-amplitude gravity anomalies. Palaeomagnetic studies on the Bushveld Complex should also factor in flattening of the entire complex, southward movement of its central parts and the approximately 35° anticlockwise rotation of the Burgersfort Bulge and central portions of the main chamber.

12. Conclusion

What would be the geometry of a “restored” Bushveld Complex, with most of its cumulative strain, displacement and rotation of various components removed? On a macroscale, along its NNW-SSE axis, the regional asymmetry of the main chamber would be reduced; i.e. the steepness of its northern edge, which is a response to deformation and approximately 10 km of uplift along TML, Zebediela, Welgevonden/Southern and Bobejaanswater Fault system(s), much of the strain that resulted in the complex's initial N–S flattening, and the lateral escape of the Burgersfort Bulge, would be removed. In order to restore the northern edge of the main chamber of the complex, southward vergence or thrusting and a minimum of 70 km southward offset cause by the Droogekloof Thrust, Boschpoort Fault/Thrust and Southern Boundary Fault to the S/SE of Thabazimbi, would have to be reversed. The significantly greater displacement of the central portion of the complex, by approximately 170 km, inferred to be due to deeper-seated, ductile, syn-cooling processes, would also have to be considered. Overlapping with this, the 35° anticlockwise rotation of the eastern and central parts of the main chamber and the Burgersfort Bulge would have to be reversed, as would extensive right-lateral offset along the Crocodile River Fault. The schematic of Fig. 10, which does not take into consideration any volume changes, attempts to illustrate these reversals.

Clockwise rotation of the Burgersfort Bulge rotates the Laersdrif Fault and other NW-SE trending faults to the SW of Booysendal into parallelism with the Crocodile River Fault (i.e. to NNW-SSE trends), while other, previously NE-SW- trending faults would revert to ENE-WSW trends (Fig. 10). The pattern that emerges is a series of ENE-WSW-trending, probably normal faults, such as the Wonderkop-Stofpoort, Dwarsrivier-Steelpoort, Klopperskloof, TML, Zebediela, Welgevonden/Southern, Bobejaanswater system(s), Ysterberg-Planknek, Sandsloot, Vlakfontein and Chaneng Faults. These are transected by a series of NNW-SSE-trending, strike-slip transverse structures such as the

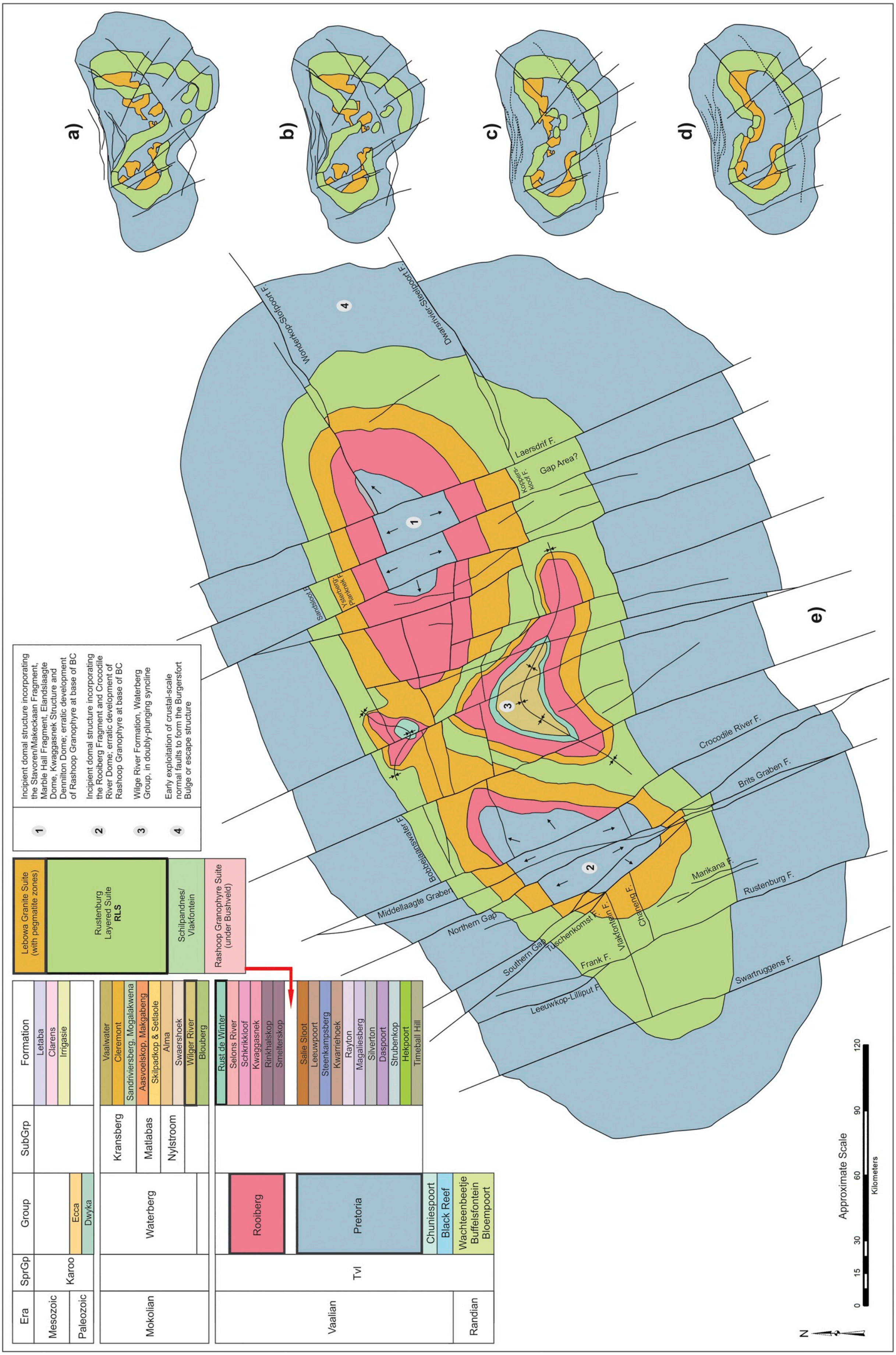

(caption on next page)

Fig. 10. Schematic of the "restored" main chamber of the Bushveld Complex (e), via a series of sub-figures (a–d) that illustrate proposed intermediate steps from its current configuration (a), using the RLS, RGS and Pretoria Group as references. The ratio of the long vs. short axes would be reduced and the lateral escape of the Burgersfort Bulge would be reversed. The asymmetry, along a N–S section, of the main chamber's northern edge would be removed, as would 70 km of southward thrusting/vergence along the Droogekloof Thrust, Boschpoort Fault/Thrust and Southern Boundary Fault to the S/SE of Thabazimbi. The cumulative offset of at least 170 km, through the central portion of the main chamber, would also be removed. The 35° anticlockwise rotation of the eastern and central parts of the main chamber, and the Burgersfort Bulge, aided by right-lateral offset along the Crocodile River Fault is restored by a concomitant 35° clockwise rotation. The latter also rotates the Laersdrif Fault - and other NW–SE trending faults - into parallelism with the Crocodile River Fault (*viz.*, to NNW-SSE trends). In the same manner, previously NE–SW-trending faults become ENE-WSW-trending. The pattern that emerges is recognizable as a series of ENE-WSW-trending, normal faults (e.g. Wonderkop-Stofpoort, Dwarsrivier-Steelpoort, Klopperskloof, TML, Zebediela, Planknek, Welgevonden/Southern, Bobejaanswater system(s), Ysterberg-Planknek, Sandsloot, Vlakfontein and Chaneng Faults), which are cross-cut by a series of NNW-SSE-trending, strike-slip, transverse faults (Laersdrift, Crocodile River, Brits Graben, Tuschenkomst, Leeuwkop, Lilliput, Frank, Rustenburg and Swartruggens). The Stavoren/Makeckaan Fragment, Marble Hall Fragment, Elandslaagte Dome, Kwaggasnek Structure and Dennilton Dome collectively revert to a position very similar to that of the Rooiberg Fragment and Crocodile River Dome, symmetrically positioned with respect to the center of the overall coverage of the main chamber and thereby defining two very early structures that occupied the deeper, central portions of each limb of the main chamber.

Laersdrift, Crocodile River, Brits Graben, Tuschenkomst, Leeuwkop, Lilliput, Frank, Rustenburg and Swartruggens Faults (Fig. 10).

The Stavoren/Makeckaan Fragment, Marble Hall Fragment, Elandslaagte Dome, Kwaggasnek Structure and Dennilton Dome collectively revert to a position very similar to that of the Rooiberg Fragment and Crocodile River Dome, symmetrically positioned with respect to overall center of the main chamber. This suggests that these features collectively formed part of two early domal structures, in trun centered on the Western and Eastern Limbs. The Wilge River Formation of the Waterberg Group moves to almost the exact center of the main chamber, within an interpreted doubly-plunging synclinal structure (Fig. 10). This combined restoration would also remove the curvature of the Southern Limb and bring its western edge back into continuity with the south-eastern termination of the Western Limb. Highly-magnetic volumes, defined by magnetic susceptibility isoshells around the Dwarsfontein Complex/Thrust Outlier and those to the north of the Wonderfontein area (Fig. 9), would become symmetrically situated at each end of the incipient Southern "Limb" and the multitude of F, Fe, Zn, Pb, Cu, Co, Mo, Ni, Ag, Au, As, Th and REE occurrences of the Enkeldoorn-Naauwpoort Houtenbek area would revert to an along-strike position with identical occurrences in the Rooiberg area.

The restoration described above only addresses the main chamber of the complex. However, in terms of a larger-scale reconstruction or reconciliation of the main chamber with the Northern Limb, the N-up vertical displacement of the Northern Limb, uplift and erosion of its western part, inward dip of the Northern Limb based on gravity data inversion work, and the effects of deformation along the TML, Zebediela, Welgevonden/Southern Faults and the Bobejaanswater Fault system(s) need to be considered. Accounting for these effects would move the eastern part of the Northern Limb eastwards and the western part of the Northern Limb westwards, while the removal of the effects of the Abbotspoort Fault System would restore the northern part of the Northern Limb to a concave-north outcrop. This would create a largely symmetrical, very flat-lying body with approximately equal N–S and E–W dimensions (320 km by 320 km). It is not unreasonable to propose that the entire complex may have exhibited a greater N–S/NNE dimension than an E–W dimension, upon its intrusion.

Acknowledgements

The author thanks Jude King, Vessela Hobson and Xpotential for gravity and magnetic data inversion work. Justine Jaguin is thanked for supplying structural data in the Murchison area. The author acknowledges M-J. McCall for helpful pointers and P. Creus and B. Stoch for assistance with inputs to several of the figures. The author thanks Rob Govers for his persistence and support throughout the editorial and review process. Patrick Eriksson and two anonymous reviewers are thanked for comments that clarified key parts of the manuscript and improved its referencing.

References

Alexandre, P., Andreoli, M.A.G., Jamison, A., Gibson, R.L., 2006. $^{40}Ar/^{39}Ar$ age constraints on low grade metamorphism and cleavage development in the Transvaal Supergroup (central Kaapvaal Craton, South Africa): implications for the tectonic setting of the Bushveld Igneous Complex. S. Afr. J. Geol. 109, 393–410.
Andreoli, M.A.G., 1988a. The discovery of a hidden and strange African orogeny: the Transvaalide Fold Belt. In: Tectonic Division of the Geological Society of South Africa Abstracts Volume, 4th Annual Conferencepp. 1–2.
Andreoli, M.A.G., 1988b. Evidence for thrust tectonics in the Transvaal Sequence based on geophysical profiles. In: Extended Abstracts, Geocongress '88, Geological Society of South Africapp. 3–6.
Armit, R.J., Ailleres, L., Baines, A.G., Betts, P.G., 2010. Understanding the limitations provided by unconstrained potential-field inversions on 3D models: a case study from the Mount Painter Inlier, SA. In: Geo-Computing 2010 Conference, Brisbane, September 2010, AIG Bulletin No. 49.
Ashwal, L.D., Webb, S.J., Knoper, M.W., 2005a. Magmatic stratigraphy in the Bushveld northern lobe: continuous geophysical and mineralogical data from the 2950 m Bellevue drillcore. S. Afr. J. Geol. 108, 132–199.
Ashwal, L.D., Webb, S.J., Knoper, M.W., 2005b. Physical and mineralogical properties of Bushveld rocks: magnetic susceptibility, density and mineral chemistry profiles in the 2950 m Bellevue drillcore, Northern Lobe. S. Afr. J. Geol. 108 (2), 199–232.
Babayeju, O.K.T., 1999. Geophysical Investigation of the Marble Hall Fragment of the Bushveld Complex. Unpub. M.Sc. Thesis. University of Pretoria, pp. 115.
Bamisaiye, O.A., Eriksson, P.G., Van Rooy, J.L., Brynard, H.M., Foya, S., Billay, A.Y., Nxumalo, V., 2017. Subsurface mapping of Rustenburg Layered Suite (RLS), Bushveld Complex, South Africa: Inferred structural features using borehole data and spatial analysis. J. Afr. Earth Sci. 132, 139–167.
Bartlett, P.J., 1994. In: Anhaeusser, C.R. (Ed.), Geology of the Premier Diamond Pipe. vol. 3. XVth CMMI Congress, South African Institute of Mining and Metallurgy, Johannesburg, South Africa, pp. 201–213.
Basson, I.J., Koegelenberg, C., 2017. Structural controls on Fe mineralization at Thabazimbi Mine, South Africa. Ore Geol. Rev. 80, 1056–1071.
Basson, I.J., Lourens, P., Paetzold, H.-D., Thomas, S., Brazier, R., Molabe, P., 2017. Structural analysis and 3D modelling of major mineralizing structures at the Phalaborwa copper deposit. Ore Geol. Rev. 83, 30–42.
Bastin, H.A., 1968. Zur Tectonic Und Stratigraphie Am Nord-iJstlichen Bushveld-Rand. Ph.D. thesis (unpubl.). Technische Hochschule, Aachen, pp. 52.
Blain, M.R., 1975. The occurrence of andalusite in the metamorphic aureole of the Bushveld Complex in the Eastern Transvaal. In: Unpub. Report of the Geological Survey of South Africa, 0103.
Boer, R.H., Meyer, F.M., Robb, L.J., Graney, J.R., Vennemann, T.W., Kesler, S.E., 1995. Mesothermal-type mineralization in the Sabie-Pilgrim's Rest gold field, South Africa. Econ. Geol. 90 (4), 860–876.
Brandl, G., 1986. The geology of the Pietersburg area. In: Explanation Sheet Geological Survey South Africa, 2328 (Pietersburg), pp. 43.
Brock, B.B., 1957. World patterns and lineaments. Trans. Geol. Soc. S. Afr. 59, 147–194.
Buchanan, D.L., 1975. The petrography of the Bushveld Complex intersected by boreholes in the Bethal area. Trans. Geol. Soc. S. Afr. 78, 335–348.
Buick, I.S., Maas, R., Gibson, R., 2001. Precise U-Pb titanite age constraints on the emplacement of the Bushveld Complex, South Africa. J. Geol. Soc. Lond. 158, 3–6.
Buick, I.S., Stevens, G., Gibson, R.L., 2004. The role of rater retention in the anatexis of metapelites in the Bushveld Complex aureole, South Africa: an experimental study. J. Petrol. 45 (9), 1777–1797.
Bumby, A., Eriksson, P.G., van de Merwe, R., 1998. Compressive deformation in the floor rocks to the Bushveld Complex (South Africa): evidence from the Rustenburg Fault Zone. J. Afr. Earth Sci. 27 (3), 307–330.
Burke, K., Dewey, J.F., 1973. Plume-generated triple junctions: key indicators in applying plate tectonics to old rocks. J. Geol. 81, 406–433.
Button, A., 1973. A Regional Study of the Stratigraphy and Development of the Transvaal Basin in the Eastern and Northeastern Transvaal. Unpub. Ph.D. thesis. Univ. Witwatersrand, Johannesburg, pp. 352.
Button, A., 1976. Stratigraphy and relations of the Bushveld floor in the eastern Transvaal. Trans. Geol. Soc. S. Afr. 79, 3–12.
Bye, A.R., Bell, F.G., 2001. Stability assessment and slope design at Sandsloot open pit, South Africa. Int. J. Rock Mech. Min. Sci. 38, 449–466.

Bye, A.R., Mossop, D., 2005. Slope stability risk management at Anglo Platinum's Sandsloot Open Pit. In: Institute of Quarrying's 36th Annual Conference and Exhibitionpp. 25.

Campbell, G., 2011. Exploration geophysics of the Bushveld Complex in South Africa. The Leading Edge, Society of Exploration Geophysicists 30 (6), 622–638.

Carr, H.W., Groves, D.I., Cawthorn, R.G., 1994. The importance of syn-magmatic deformation in the formation of the Merensky Reef potholes in the Bushveld Complex. Econ. Geol. 89, 1398–1410.

Cawthorn, R.G., 1998. Geometrical relations between the Transvaal Supergroup, the Rooiberg Group, and the mafic rocks of the Bushveld Complex. S. Afr. J. Geol. 101, 275–279.

Cawthorn, R.G., 1999. The platinum and palladium resources of the Bushveld Complex. S. Afr. J. Sci. 95, 481–489.

Cawthorn, R.G., 2013. The Residual or Roof Zone of the Bushveld Complex, South Africa. J. Petrol. 54 (9), 1875–1900.

Cawthorn, R.G., Barnes, S.J., Ballhaus, C., Malitch, K.N., 2005. Platinum-group element, chromium, and vanadium deposits in mafic and ultramafic rocks. In: Economic Geology, 100th Anniversary Volume, pp. 215–249.

Cawthorn, R.G., Cooper, G.R.J., Webb, S.J., 1998. Connectivity between the Western and Eastern Limbs of the Bushveld Complex. S. Afr. J. Geol. 101, 291–298.

Cawthorn, R.G., Eales, H.V., Walraven, F., Uken, R., Watkeys, M.K., 2006. The Bushveld Complex. In: Johnson, M.R., Anhaeusser, C.R., Thomas, R.J. (Eds.), The Geology of South Africa. Geological Society of South Africa. Johannesburg/Council for Geoscience, Pretoria, pp. 261–281.

Cawthorn, R.G., McKenna, N., 2006. The extension of the Western Limb, Bushveld Complex (South Africa), at Cullinan Diamond Mine. Mineral. Mag. 70 (3), 241–256.

Cawthorn, R.G., Meyer, P.S., Kruger, F.J., 1991. Major addition of magma at the Pyroxenite Marker in the Western Bushveld Complex, South-Africa. J. Petrol. 32, 739–763.

Cawthorn, R.G., Spies, L., 2003. Plagioclase content of cyclic units in the Bushveld Complex, South Africa. Contrib. Mineral. Petrol. 145, 47–60.

Cawthorn, R.G., Walraven, F., 1998. Emplacement and crystallization time for the Bushveld Complex. J. Petrol. 39, 1669–1687.

Cawthorn, R.G., Webb, S.J., 2001. Connectivity between the Western and Eastern Limbs of the Bushveld Complex. Tectonophysics 330, 195–209.

Cheney, E.S., Twist, D., 1991. The conformable emplacement of the Bushveld Mafic rocks along a regional unconformity in the Transvaal Succession of South Africa. Precambrian Res. 52, 115–132.

Clark, R.J., 1972. The Geology of the Roodekraal Igneous Complex. Potchefstroom District. Unpub. M.Sc. dissertation. University of the Witwatersrand, South Africa, pp. 137.

Clarke, B.M., Uken, R., Watkeys, M.K., 2000. Intrusion mechanisms of the southwestern Rustenburg Layered suite as deduced from the Spruitfontein inlier. S. Afr. J. Geol. 103, 120–127.

Clarke, B.M., Uken, R., Watkeys, M.K., Reinhardt, J., 2005. Folding of the Rustenburg Layered Suite adjacent to the Steelpoort pericline: implications for syn-Bushveld tectonism in the eastern Bushveld Complex. S. Afr. J. Geol. 108, 395–410.

Clarke, B.M., Uken, R., Watkeys, M.K., Reinhardt, J., 2009. Structural and compositional constraints on the emplacement of the Bushveld Complex, South Africa. Lithos 111, 21–36.

Clubley-Armstrong, A.R., Sharpe, M.R., 1979. The structural evolution of the Dennilton Dome and its relationship to the intrusion of the Bushveld Complex. Trans. Geol. Soc. S. Afr. 82, 23–36.

Coetzee, F.J., 1958. Intrusive relationship and ore deposits in the western part of the Bushveld Igneous Complex. Trans. Geol. Soc. S. Afr. 61, 387–392.

Coetzee, F.J., 1970. The geology of the western part of the Bushveld Igneous Complex. Special Publication of the Geological Society of South Africa 1, 1–20.

Cole, J., Finn, C.A., Webb, S.J., 2013. Overview of the magnetic signatures of the Palaeoproterozoic Rustenburg Layered Suite, Bushveld Complex, South Africa. Precambrian Res. 236, 193–213.

Cole, J., Webb, S.J., Finn, C.A., 2014. Gravity models of the Bushveld Complex - have we come full circle? J. Afr. Earth Sci. 92, 97–118.

Coomber, S.J., 2008. Gravity Modelling in the Western Bushveld Complex, South Africa, Using Integrated Geophysical Data. Unpub. M.Sc. Thesis. University of the Witwatersrand, pp. 237.

Council for Geoscience, 1997. Gravity Map of South Africa, 1:1,000,000 Map Series.

Cousins, C.A., 1959. The structure of the mafic portion of the Bushveld Igneous Complex. Trans. Geol. Soc. S. Afr. 62, 174–189.

Cousins, C.A., Feringa, G., 1964. In: Haughton, S.H. (Ed.), The Chromite Deposits of the Western Belt of the Bushveld Complex. The Geology of Some Ore Deposits in Southern Africa, II. Geological Society of South Africa, Johannesburg, pp. 183–202.

Couto, P.M., Theron, W., 2014. Flexural slip thrust faulting on Booysendal Platinum Mine and the implications for rock engineering. In: The 6th International Platinum Conference, 'Platinum-Metal for the Future'. The Southern African Institute of Mining and Metallurgy, 2014.

Davis, M.D., Wilson, A.H., van der Merwe, A.J., 2007. The use of density as a stratigraphic and correlative tool for the Bushveld Complex, South Africa. In: Milkereit, B. (Ed.), Proceedings of Exploration 07: Fifth Decennial International Conference on Mineral Exploration. Decennial Mineral Exploration Conferences, Torontopp. 1193–1197.

de Kock, M.O., Ernst, R., Söderlund, U., Jourdan, F., Hofmann, A., Le Gall, B., Bertrand, H., Chisonga, B.C., Beukes, N., Rajesh, H.M., Moseki, L.M., Fuchs, R., 2014. Dykes of the 1.11 Ga Umkondo LIP, Southern Africa: Clues to a complex plumbing system. Precambrian Res. 249, 129–143.

De Waal, S.A., 1970. Interference-folding of Bushveld-Igneous-Complex age in the Transvaal System north of Marble Hall, Transvaal. In: Symposium on the Bushveld Igneous Complex and other layered intrusions. Geological Society South Africa, Special Publication 1, 283–298.

De Waal, S.A., Graham, I.T., Armstrong, R.A., 2006. The Lindeques Drift and Heidelberg Intrusions and the Roodekraal Complex, Vredefort, South Africa: co-magmatic plutonic and volcanic products of a 2055 Ma ferrobasaltic magma. S. Afr. J. Geol. 109, 279–300.

De Waal, S.A., Maier, W.D., Armstrong, R.A., Gauert, C.D.K., 2001. Parental magma and emplacement of the stratiform Uikomst complex, South Africa. Can. Mineral. 39 (2), 557–571. https://doi.org/10.2113/gscanmin.39.2.557.

Du Plessis, A., Clendenan, C.W., 1988. The Bobbejaanwater Fault System south of Thabazimbi, western Transvaal. S. Afr. J. Geol. 91 (1), 97–105.

Du Plessis, A., Kleywegt, R.J., 1987. A dipping sheet model for the mafic lobes of the Bushveld Complex. Trans. Geol. Soc. S. Afr. 90, 1–6.

Du Plessis, C.P., 1987. New perspectives on early Waterberg Group sedimentation from the Gatkop area, northwestern Transvaal. S. Afr. J. Geol. 90, 395–408.

Du Plessis, C.P., Walraven, F., 1990. The tectonic setting of the Bushveld Complex in Southern Africa, part 1. Structural deformation and distribution. Tectonophysics 179, 305–319.

Dube, Z.A., 2010. The Merensky Reef and UG2 layers at De Wildt, Western Limb of the Bushveld Complex. Unpub. M.Sc. Thesis. University of the Witwatersrand, Johannesburg, pp. 144.

Eales, H.V., Botha, W.J., Hattingh, P.J., de Klerk, W.J., Maier, W.D., Odgers, A.T.R., 1993. The mafic rocks of the Bushveld Complex: a review of emplacement and crystallization history, and mineralization, in the light of recent data. Journal of African Earth Sciences (and the Middle East) 16 (1–2), 121–142.

Eales, H.V., Cawthorn, R.G., 1996. The Bushveld complex. In: Cawthorn, R.G. (Ed.), Layered Intrusions. Elsevier, Amsterdam, pp. 181–230.

Engelbrecht, I.P., 1988. Die Bosveld Komplex en sy Vloergesteentes in die omgewing van Nietverdiend Wes-Transvaal. Ph.D. thesis (unpub1.). Univ. of Pretoria, pp. 327.

Eriksson, P.G., Altermann, W., Catuneanu, O., van der Merwe, R., Bumby, A., 2001. Major influences on the evolution of the 2.67–2.1 Ga Transvaal basin, Kaapvaal craton. Sediment. Geol. 141-142, 205–231.

Eriksson, P.G., Hatting, P.J., Altermann, W., 1995. An overview of the geology of the Transvaal Sequence and Bushveld Complex, South Africa. Mineral. Deposita 30 (2), 98–111.

Eriksson, P.G., Reczko, B.F.F., 1995. The sedimentary and tectonic setting of the Transvaal Supergroup floor rocks to the Bushveld Complex. J. Afr. Earth Sci. 21, 487–504.

Eriksson, P.G., Schreiber, U.M., Van der Neut, M., 1991. A review of the sedimentology of the Early Proterozoic Pretoria Group, Transvaal Sequence, South Africa. Implications for tectonic setting. J. Afr. Earth Sci. 13, 107–119.

Ernst, R., 2014. Plumbing system of LIPs. In: Large Igneous Provinces. Cambridge University Press, Cambridge. https://doi.org/10.1017/CBO9781139025300.005, 111-153.

Ferré, E.A., Wilson, J., Gleizes, G., 1999. Magnetic susceptibility and AMS of the Bushveld alkaline granites, South Africa. Tectonophysics 307 (1–2), 113–133.

Finn, C.A., Bedrosian, P.A., Cole, J.C., Khoza, T.D., Webb, S.J., 2015. Mapping the 3D extent of the Northern Lobe of the Bushveld layered mafic intrusion from geophysical data. Precambrian Res. 268, 279–294.

Frick, C., Walraven, F., 1985. The petrology and geochemistry of the pre: Karoo Elandskraal Volcano, South Africa. Trans. Geol. Soc. S. Afr. 88, 225–243.

Fullagar, P.K., Pears, G.A., 2007. In: Milkereit, B. (Ed.), Towards Geologically Realistic Inversion. Proceedings of Exploration 07: Fifth Decennial International Conference on Mineral Exploration, vol. 2007. pp. 444–460.

Gauert, C.D.K., 1998. The Petrogenesis of the Uitkomst Complex, Mpumalanga Province, South Africa. PhD Thesis (unpubl.). University of Pretoria, Pretoria.

Gauert, C.D.K., 2001. Sulphide and oxide mineralisation in the Uikomst Complex, South Africa: origin in a magma conduit. J. Afr. Earth Sci. 32 (2), 149–161.

Gauert, C.D.K., De Waal, S.A., Wallmach, T., 1995. Geology of the ultrabasic to basic Uitkomst complex, eastern Transvaal, South Africa: an overview. J. Afr. Earth Sci. 21 (4), 553–570.

Gauert, C.D.K., Jordaan, L.D., De Waal, S.A., Wallmach, T., 1996. Isotopic constraints on the source of the sulphur for the base metal sulphides of the Uitkomst Complex, Badplaas, South Africa. S. Afr. J. Geol. 99, 41–50.

Gauert, C.D.K., Kotzé, E., Beukes, J.J., Giebel, R.J., 2013. Reef disturbances of Critical Zone rocks of the eastern Bushveld Complex in the vicinity of the Steelpoort fault, South Africa - petrogenetic implications. In: Jonsson, E. (Ed.), Mineral Deposit Research for a High-tech World. Proceedings of the 12th Biennial SGA meeting, Uppsala, Sweden, vol. 3. pp. 989–992.

Geological Survey of South Africa, 1974. 2426 Thabazimbi 1:250,000. Geological Map Series.

Geological Survey of South Africa, 1978a. 2428 Nylstroom 1:250,000. Geological Map Series.

Geological Survey of South Africa, 1978b. 2528 Pretoria 1:250,000. Geological Map Series.

Geological Survey of South Africa, 1981. 2526 Rustenburg 1:250,000. Geological Map Series.

Geological Survey of South Africa, 1985. 2328 Pietersburg 1:250,000. Geological Map Series.

Gerya, T.V., Uken, R., Reinhardt, J., Watkeys, M.K., Maresch, W.V., Clarke, B.M., 2003. Cold fingers in a hot magma: Numerical modeling of country rock diapirs in the Bushveld Complex, South Africa. Geology 31, 753–756.

Gerya, T.V., Uken, R., Reinhardt, J., Watkeys, M.K., Maresch, W.V., Clarke, B.M., 2004. "Cold" diapirs triggered by intrusion of the Bushveld Complex: Insight from two-dimensional numerical modeling. In: Whitney, D.L., Teyssier, C., Siddoway, C.S. (Eds.), Gneiss Domes in Orogeny: Boulder, Colorado, Geological Society of America Special Paper 380, pp. 117–127.

Gibson, R.L., Courtnage, P.M., Charlesworth, E.G., 1999. Bedding-parallel shearing and related deformation in the lower Transvaal Supergroup north of the Johannesburg Dome, South Africa. S. Afr. J. Geol. 102 (2), 99–108.
Good, N., De Wit, M.J., 1997. The Thabazimbi-Murchison lineament of the Kaapvaal Craton, South Africa: 2700 ma of episodic deformation. J. Geol. Soc. Lond. 154, 93–97.
Greyvensteyn, R.M., 2001. A GIS-Based Structural Analysis of the Bushveld Complex and Surrounding Areas. Unpub. M.Sc. Thesis, University of Pretoria, pp. 199.
Gumsley, A., Rådman, J., Söderlund, U., Klausen, M., 2016. U–Pb baddeleyite geochronology and geochemistry of the White Mfolozi Dyke Swarm: unravelling the complexities of 2.70–2.66 Ga dyke swarms across the eastern Kaapvaal Craton, South Africa. GFF. https://doi.org/10.1080/11035897.2015.1122665.
Hall, A.L., 1932. The Bushveld Igneous Complex of the Central Transvaal. Mem. Geol. Surv. S. Afr. 28, 560.
Hanson, R.E., Gose, W.A., Crowley, J.L., Ramezani, J., Bowring, S.A., Bullen, D.S., Hall, R.P., Pancake, J.A., Mukwakeami, J., 2004. Paleoproterozoic intraplate magmatism and basin development on the Kaapvaal Craton: age, paleomagnetism and geochemistry of ∼1.93 to ∼1.87 Ga post-Waterberg dolerites. S. Afr. J. Geol. 107, 233–254.
Harding, T.P., 1985. Seismic characteristics and identification of negative flower structures, positive flower structures, and positive structural inversion. Bull. Am. Assoc. Pet. Geol. 69 (4), 582–600.
Hardwick, B.W., Jowitt, S.M., Keays, R.R., 2015. Controls on disseminated PGE-Cu-Ni sulfide mineralization within the Rietfontein deposit, Eastern Limb, Bushveld Complex, South Africa: implications for the formation of contact-type magmatic sulfide deposits. Ore Geol. Rev. 64, 253–272.
Harley, M., Charlesworth, E.G., 1992. Thrust-controlled gold mineralisation at the Elandshoogte Mine, Sabie-Pilgrim's Rest goldfield, South Africa. Mineral. Deposita 27 (2), 122–128.
Harley, M., Charlesworth, E.G., 1993. Controls and Structural Development of Epigenetic Mesothermal Gold Mineralization in the Sabie-Pilgrim's Rest Goldfield, Eastern Transvaal, South Africa. University of the Witwatersrand Economic Geology Research Unit, Information Circular 268.
Harley, M., Charlesworth, E.G., 1996. The role of fluid pressure in the formation of bedding-parallel, thrust-hosted gold deposits, Sabie-Pilgrim's Rest goldfield, eastern Transvaal. Precambrian Res. 79, 125–140.
Harmer, R.E., Armstrong, R.A., 2000. Duration of Bushveld Complex (*sensu lato*) magmatism: constraints from new SHRIMP zircon chronology. In: Workshop on the Bushveld Complex. University of the Witwatersrand, Johannesburg, Gethane Lodge, Burgersfort.
Harper, F., Clay, A.N., De Wit, D.R., 2009. National instrument 43–101 Technical Report and Valuation Statement for the Loskop Project, Mpumalanga Province, South Africa, for Platmin Limited. Report No. D584R - Loskop by Venmyn. pp. 77.
Harris, N., McMillan, A., Holness, M., Uken, R., Watkeys, M., Rogers, R., Fallick, A., 2003. Melt generation and fluid flow in the thermal aureole of the Bushveld Complex. J. Petrol. 44 (6), 1031–1054.
Hartzer, F.J., 1987. Die Geologie van die Krokodilrivier Fragment. Thesis, Rand Afrikaans University, Unpub. M.Sc, pp. 201.
Hartzer, F.J., 1995. Transvaal Supergroup inliers: geology, tectonic development and relationship with the Bushveld Complex, South Africa. J. Afr. Earth Sci. 21, 521–547.
Hattingh, P.J., 1977. 'n Regionale Gravitasie-opname van die Bosveldkompleks in die Omgewing van Groblersdal, Lydenburg en Belfast. Unpub. M.Sc. Thesis. University of Pretoria.
Hattingh, P.J., 1986. The paleomagnetism of the Merensky reef footwall rocks of the Bushveld Complex. Trans. Geol. Soc. S. Afr. 89, 1–8.
Hattingh, P.J., 1991. The magnetic susceptibility of the mafic rocks of the Bushveld Complex. S. Afr. J. Geol. 94, 132–136.
Hatton, C.J., Schweitzer, J.K., 1995. Evidence for synchronous extrusive and intrusive Bushveld magmatism. J. Afr. Earth Sci. 21, 579–594.
Hayes, B., Ashwal, L.D., Webb, S.J., Bybee, G.M., 2017a. Large-scale magmatic layering in the Main Zone of the Bushveld Complex and episodic downward magma infiltration. Contrib. Mineral. Petrol. 172 (2–3), 1–13.
Hayes, B., Bybee, G.M., Nex, P.A.M., Van Niekerk, D., 2017b. Discordant Intra-mush Channels and Expulsion of Residual Melts From the Layered Sequence of the Bushveld Complex. AGU 2017 Fall Meeting, New Orleans.
Hemant, K., 2003. Modelling and Interpretation of Global Lithospheric Magnetic Anomalies. Unpub. Dissertation. Freien Universität Berlin, pp. 137.
Hilliard, P., McCourt, S., 1995. Bedding-parallel simple shear deformation in the West Rand Group rocks on Northcliff Promontory, Johannesburg. South Africa; insight into the late Archaean evolution of the Kaapvaal Craton. S. Afr. J. Geol. 98, 349–355.
Holzer, L., Frei, R., Barton, J.M., Kramers, J.D., 1998. Unravelling the record of successive high grade events in the Central Zone of the Limpopo Belt using Pb single phase dating of metamorphic minerals. Precambrian Res. 87, 87–115.
Hornsey, R.A., 1999. The Genesis and Evolution of the Nkomati Mine Ni-sulphide deposit, Mpumalanga Province, South Africa. Unpub. M.Sc. thesis. Dept. of Geology and Applied Geology, University of Natal, Durban, pp. 224.
Hunter, D.R., 1975. The Regional Geologic Setting of the Bushveld Complex (An adjunct to the provisional tectonic map of the Bushveld Complex). Economic Geology Research Unit, University of the Witwatersrand, pp. 18.
Hunter, D.R., 1976. Some enigmas of the Bushveld Complex. Econ. Geol. 71, 229–248.
Hunter, D.R., Hamilton, P.I., 1978. The Bushveld Complex. In: Tarling, D.H. (Ed.), Evolution of the Earth's Crust. Academic Press, London, pp. 103–107.
Hunter, D.R., Reid, D.L., 1987. Mafic dyke swarms in southern Africa. In: Hall, H.C., Fahrig, W.F. (Eds.), Mafic Dyke Swarms Volume. Geological Association of Canada Special Paper. vol. 34. pp. 445–456.
Huthmann, M.A., Yudovskaya, M.A., Kinnaird, J.A., 2016. Geochronological evidence for an extension of the Northern Lobe of the Bushveld Complex, Limpopo Province, South Africa. Precambrian Res. 280, 61–75.
Ireland, R.H.P., Penniston-Dorland, S.C., 2015. Chemical interactions between a sedimentary diapir and surrounding magma: evidence from the Phepane Dome and Bushveld Complex, South Africa. Mineralogical Society of America 100 (8–9), 1985–2000.
Jaguin, J., Gapais, D., Poujol, M., Boulvais, P., Moyen, J.F., 2012. The Murchison Greenstone Belt (South Africa): a general tectonic framework. S. Afr. J. Geol. 115 (1), 65–76.
Jansen, H., Schifano, G., Schutte, I.C., 1974. Geological map with explanatory notes. In: 1:250,000 Geological Series 2426 Thabazimbi. Geological Survey of South Africa, Pretoria (Compilers).
Johnson, T., Brown, M., Gibson, R., Wing, B., 2004. Spinel-cordierite symplectites replacing andalusite: evidence for melt assisted diapirism in the Bushveld Complex, South Africa. J. Metamorph. Geol. 22 (6), 529–545.
Jones, M.Q.W., 2015. Thermophysical properties of rocks from the Bushveld Complex. J. South. Afr. Inst. Min. Metall. 115 (2), 153–160.
Joubert, P.L., Gauert, C., Davidson, M., Van Lente, B., 2006. Syn- to post-intrusive deformation in the chromitiferous harzburgite, Uitkomst Complex, South Africa. In: Colloquium of African Geology 21 Abstracts. vol. 1 (Maputo, Mozambique).
Kamber, B.S., Kramers, J.D., Napier, R., Cliff, R.A., Rollinson, H.R., 1995. The Triangle shear zone, Zimbabwe, revisited, new data document an important event at 2.0 Ga in the Limpopo Belt. Precambrian Res. 70, 191–213.
Kamo, S.L., Reimold, W.U., Krogh, T.E., Colliston, W.P., 1996. A 2.023 Ga age for the Vredefort impact event and a first report of shock metamorphosed zircons in pseudotachylite breccias and granophyre. Earth Planet. Sci. Lett. 144, 369–388.
Kent, L.E., 1957. Discussion of paper by B.B. Brock (1957). Trans. Geol. Soc. S. Afr. 60, 163–172.
Kgaswane, E.M., Nyblade, A.A., Durrheim, R.J., Julià, J., Dirks, P.H.G.M., Webb, S.J., 2012. Shear wave velocity structure of the Bushveld Complex, South Africa. Tectonophysics 554–557, 83–104.
Kgaswane, E.M., Nyblade, A.A., Julià, J., Dirks, P.H.G.M., Durrheim, R.J., Pasyanos, M.E., 2009. Shear wave velocity structure of the lower crust in southern Africa: evidence for compositional heterogeneity within Archaean and Proterozoic terrains. J. Geophys. Res. 114 (B12), B12304.
Kinnaird, J.A., Hutchinson, D., Schurmann, L.W., Nex, P.A.M., De Lange, R., 2005. Petrology and mineralisation of the southern Platreef: Northern Limb of the Bushveld Complex, South Africa. Mineral. Deposita. https://doi.org/10.1007/s00126-005-0023-9.
Kinnaird, J.A., McDonald, I., 2005. An introduction to mineralisation in the Northern Limb of the Bushveld Complex. Applied Earth Science: Transactions of the Institutions of Mining and Metallurgy: Section B 114 (4), 194–198.
Kinnaird, J.A., Yudovskaya, M., McCreesh, M., Huthmann, F., Botha, T.J., 2017. The Waterberg platinum group element deposit: Atypical mineralization in mafic-ultramafic rocks of the Bushveld Complex, South Africa. Econ. Geol. 112, 1367–1394.
Klausen, M.B., Söderlund, U., Olsson, J.R., Ernst, R.E., Armoogam, M., Mkhize, S.W., Petzer, G., 2010. Petrological discrimination among Precambrian dyke swarms: Eastern Kaapvaal craton (South Africa). Precambrian Res. 183 (2010), 501–522.
Kleywegt, R.J., Du Plessis, A., 1986. On the structure of the Bushveld Complex and the central Transvaal basin. In: Extended Abstracts, Geocongress '86, Univ. of the Witwatersrand, Johannesburg, S. Afr.
Kruger, F.J., 2005. Filling the Bushveld Complex magma chamber: lateral expansion, roof and floor interaction, magmatic unconformities, and the formation of giant chromitite, PGE and Ti-V-magnetitite deposits. Mineral. Deposita 40 (5), 451–472.
Ledwaba, L., Dingoko, O., Cole, P., Havenga, M., 2009. Compilation of survey specifications for all the old regional airborne geophysical surveys conducted over South Africa. In: Council for Geoscience Report, pp. 40.
Lee, C.A., 1981. Post-deposition structures in the Bushveld Complex mafic sequence. J. Geol. Soc. Lond. 138, 327–341.
Lee, S.-A., 2016. Geophysical Investigation into the Geology, Geometry and Geochronology of the South African Pilanesberg Complex and Pilanesberg Dyke System. Unpub. M.Sc. Thesis. University of the Witwatersrand, pp. 250.
Lenhardt, N., Eriksson, P.G., 2012. Volcanism of the Palaeoproterozoic Bushveld Large Igneous Province: The Rooiberg Group, Kaapvaal Craton, South Africa. Precambrian Research, (special volume for Wulf Mueller). pp. 1–47.
Letts, S., Torsvik, T.H., Webb, S., Ashwal, L.D., 2009. Palaeomagnetism of the 2054 Ma Bushveld Complex (South Africa): Implications for emplacement and cooling. Geophys. J. Int. 179, 850–872.
Letts, S., Torsvik, T.H., Webb, S.J., Ashwal, L.D., 2011. New Palaeoproterozoic palaeomagnetic data from the Kaapvaal Craton, South Africa. Geol. Soc. Lond., Spec. Publ. 357, 9–26.
Letts, S., Torsvik, T.H., Webb, S.J., Ashwal, L.D., Eide, E.A., Chunnett, G., 2005. Palaeomagnetism and $^{40}Ar/^{39}Ar$ geochronology of mafic dykes from the eastern Bushveld Complex (South Africa). Geophys. J. Int. 162, 36–48.
Li, Y., Oldenburg, D.W., 1996. 3-D inversion of magnetic data. Geophysics 61, 394–408.
Li, Y., Oldenburg, D.W., 1998. 3-D inversion of gravity data. Geophysics 63, 109–119.
Liebenberg, L., 1970. The sulphides in the layered sequence of the Bushveld igneous complex. In: Visser, D.J.L., von Gruenewaldt, G. (Eds.), Symposium on the Bushveld Complex and other Layered Intrusions. Geological Society of South Africa Special Publication Ipp. 108–207.
Longridge, L., Gibson, R., Nex, P.A.M., 2009. Structural controls on melt segregation and migration related to the formation of the diapiric Schwerin Fold in the contact aureole of the Bushveld Complex, South Africa. Earth Environ. Sci. Trans. R. Soc. Edinb. 100 (1–2), 61–76.
Maier, W.D., Karykowskia, B.T., Yang, S.-H., 2016. Formation of transgressive anorthosite seams in the Bushveld Complex via tectonically induced mobilisation of plagioclase-

rich crystal mushes. Geosci. Front. 7 (6), 875–889.
Martin, D.McB., Charlesworth, E.G., Clendenin, C.W., Maske, S., De Gasparis, A.A., 1988. The nature and influences of the Thabazimbi-Murchison Line, west of Thabazimbi, on a number of Early Proterozoic basins. In: Ext. Abstr., Geocongress '88, 22nd Earth Science Congress, Geol. Soc. S. Afr., Durbanpp. 383–386.
Martin, L.E., 1999. The Attenuation of the Main Zone at the Phosiri Dome, Bushveld Complex. M.Sc. University of the Witwatersrand, pp. 111.
Martini, J.E.J., 1998. The Loskop Formation and its relationship to the Bushveld Complex, South Africa. J. Afr. Earth Sci. 27 (2), 193–222.
Mathez, E.A., Van Tongeren, J.A., Schweitzer, J., 2013. On the relationships between the Bushveld Complex and its felsic roof rocks, part 1: petrogenesis of Rooiberg and related felsites. Contrib. Mineral. Petrol. 166, 435–449.
McCall, M.-J., 2016. Mineralogical and Geochemical Variations in the UG2 Reef at Booysendal and Zondereinde Mines, with Implications for Beneficiation of PGM. Unpub. M.Sc.. University of Stellenbosch, pp. 150.
McDonald, I., Harmer, R.E., Holwell, D.A., Hughes, H.S.R., Boyce, A.J., 2017. Cu-Ni-PGE mineralisation at the Aurora Project and potential for a new PGE province in the Northern Bushveld Main Zone. Ore Geol. Rev. 80, 1135–1159.
McKechnie, W.F., Egerton, F., Miles, J., 2015. Competent persons report for Sibanye Gold Limited on Rustenburg Operations. In: Report Prepared by Snowden and DRA, pp. 326.
Meinster, B., 1974. Thrusting and block-faulting around Gatkop east of Thabazimbi. Transvaal. Annals of the Geological Survey of South Africa 10, 57–72.
Merkle, R.K.W., 1992. Platinum-group minerals in the middle group of chromitite layers at Marikana, western Bushveld Complex: indications for collection mechanisms and postmagmatic modification. Can. J. Earth Sci. 29, 209–221.
Meyer, R., De Beer, H., 1987. Structure of the Bushveld Complex from resistivity measurements. Nature 325, 610–612.
Miyano, T., Beukes, N.J., 1987. Phase relations of stilpnomelane, ferri-annite, and riebeckite in very low grade metamorphosed iron formations. Trans. Geol. Soc. S. Afr. 87, 111–124.
Miyano, T., Beukes, N.J., Van Reenen, D.D., 1987. Metamorphic evidence for early post-Bushveld sills in the Penge Iron Formation, Transvaal Sequence, eastern Transvaal. S. Afr. J. Geol. 90, 37–43.
Moen, H.F.G., 1989. A petrographical study of Bushveld-type rocks from boreholes on the Moloto geophysical anomaly, northeast of Pretoria. S. Afr. J. Geol. 92, 84–94.
Molyneux, T.G., 1974. A geological investigation of the Bushveld Complex in Sekhukhuneland and part of the Steelpoort valley. Trans. Geol. Soc. S. Afr. 77, 329–338.
Molyneux, T.G., 2008. Compilation on a scale of 1:50,000 of the Geology of the Eastern Compartment of the Bushveld Complex. Bushveld Intelligence Center, Dept of Geology, University of Pretoria, Pretoria.
Molyneux, T.G., Klinkert, P.S., 1978. A structural interpretation of part of the eastern mafic lobe of the Bushveld Complex and its surroundings. Trans. Geol. Soc. S. Afr. 81, 359–368.
Mungall, J.E., Kamo, S.L., McQuade, S., 2016. U–Pb Geochronology Documents Out-of-Sequence Emplacement of Ultramafic Layers in the Bushveld Igneous Complex of South Africa. Nature Communications 7, Article No: 13385.
Nair, S.K., Gao, S.S., Liu, K.H., Silver, P.G., 2006. Southern African crustal evolution and composition: constraints from receiver function studies. J. Geophys. Res. 111 (B2), B02304.
Nex, P.A.M., 2005. The structural setting of mineralization on Tweefontein Hill, Northern Limb of the Bushveld Complex, South Africa. Trans. Inst. Min. Metall. 114, B23–B251.
Nomade, S., Renne, P.R., Merkle, R.K.W., 2004. ^{40}Ar/^{39}Ar age constraints on ore deposition and cooling of the Bushveld Complex, South Africa. J. Geol. Soc. Lond. 161, 411–420.
Odgers, T.E., du Plessis, A., 1993. Interpretation of a regional reflection seismic survey in the north-eastern Bushveld Complex. In: Extended Abstract: 3rd SAGA Biennial Conference and Exhibition.
Odgers, T.E., Hinds, R.C., Von Gruenewalt, G., 1993. Interpretation of a seismic reflection survey across the southern Bushveld Complex. S. Afr. J. Geol. 96 (4), 205–212.
Olsson, J.R., Söderlund, U., Klausen, M.B., Ernst, R.E., 2016. U-Pb baddeleyite ages linking major Archean dyke swarms to volcanic-rift forming events in the Kaapvaal craton (South Africa), and a precise age for the Bushveld Complex. Precambrian Res. 183 (3), 490–500.
Parsons, C.F., Killick, A.M., 1990. A reassessment of the structure of the dolomite inliers south of Westonaria. S. Afr. J. Geol. 93, 438–442.
Perritt, S., Roberts, M.K.C., 2007. Flexural-slip structures in the Bushveld Complex, South Africa? J. Struct. Geol. 29 (9), 1422–1429.
Potgieter, G., 1991. Inversion tectonics along the northeastern boundary of the Transvaal basin. Precambrian sedimentary basins of Southern Africa. Terra Nova Abstracts. 32 (Suppl. 3).
Potter, R.H., 2009. Diffusion of Oxygen and Lithium Isotopes at a Contact between the Bushveld Complex and Metasedimentary Rock: Implications for the Timescale of Phepane Dome Diapirism. M.Sc. Unpub. Thesis. University of Maryland, College Park, pp. 130.
Pretorius, D.A., Brink, W.P.J., Fouche, J., 1986. The Witwatersrand basin, surface and subsurface geology and structure. In: Anhaeusser, C.R., Maske, S. (Eds.), Mineral Deposits of Southern Africa. Geol. Soc. S. Afr. Johannesburg, 2 Vols. Map Scale 1: 500,000, pp. 983–993.
Qamata, X., Steenkamp, C.J., 2016. Negotiating complex geological structures by applying new mining strategies. In: AMMSA General Meeting 27 May 2016.
Rasmussen, B., Fletcher, I.R., Muhling, J.R., Mueller, A.G., Hall, G.C., 2007. Bushveld-aged fluid flow, peak metamorphism, and gold mobilization in the Witwatersrand basin, South Africa: constraints from in situ SHRIMP U-Pb dating of monazite and xenotime. Geology 35, 931–934.
Reading, H.G., 1980. Characteristics and recognition of strike-slip systems, in: Sedimentation in Oblique-Slip Mobile Zones. In: Balance, P.F., Reading, H.G. (Eds.), Special Publication of the International Association of Sedimentology, pp. 7–26.
Reid, D.L., Basson, I.J., 2002. Iron-rich ultramafic pegmatite replacement bodies within the Upper Critical Zone, Rustenburg Layered Suite, Northam Platinum Mine, South Africa. Mineral. Mag. 66 (6), 895–914.
Rezaiea, M., Moradzadehb, A., Kalatea, A.J., Aghajania, H., Nejati, S.M., Kahoo, A.R., 2017. 3D modelling of Trompsburg Complex (in South Africa) using 3D focusing inversion of gravity data. J. Afr. Earth Sci. 130 (1–7).
Richards, R.J., 1987. A Geological Investigation of Upper Transvaal Sequence Rocks in the Northern Portion of the Rooiberg Fragment. Unpub. M.Sc.. Thesis, University of Pretoria, pp. 90.
Robb, L.J., Freeman, L.A., Armstrong, R.A., 2000. Nature and longevity of hydrothermal fluid flow and mineralisation in granites of the Bushveld Complex, South Africa. In: Barbarin, B., Stephens, W.E., Bonin, B., Bouchez, J-L. Clarke (Eds.), Fourth Hutton Symposium: The Origin of Granites and Related Rocks, Proceedings of a Symposium held in Clermont-Ferrand, France, 1999-2000.
Roberts, M.K.C., Clark-Mostert, V., 2010. Is there some commonality between the geological structures in the Bushveld Complex and the Great Dyke? In: The 4th International Platinum Conference, Platinum in Transition 'Boom or Bust', The Southern African Institute of Mining and Metallurgy, 2010.
Schiffries, C.M., Rye, D.M., 1990. Stable isotopic systematics of the Bushveld Complex: II. Constraints on hydrothermal processes in layered intrusions. Am. J. Sci. 290, 209–245.
Schiffries, C.M., Skinner, B.J., 1987. The Bushveld hydrothermal system: field and petrologic evidence. Am. J. Sci. 287, 566–595.
Schoenberg, R., Kruger, F.J., Nağler, T.F., Meisel, T., Kramers, J.D., 1999. PGE enrichment in chromitite layers and the Merensky Reef of the western Bushveld Complex; a Re-Os and Rb-Sr isotope study. Earth Planet. Sci. Lett. 172, 49–64.
Schweitzer, J.K., Güller, G., Lambert, P., de Waal, S., Kramers, P., Naidoo, T., 2009. Technical Report on the Lebowa Platinum Mine, Limpopo Province, South Africa, for Anooraq Resources Corporation. pp. 182.
Schweitzer, J.K., Hatton, C.J., De Waal, S.A., 1997. Link between the granitic and volcanic rocks of the Bushveld Complex, South Africa. African Journal of Earth Sciences 24, 95–104.
Schwellnus, J.S.I., 1956. The Basal Portion of the Bushveld Igneous Complex and the Adjoining Metamorphosed Sediments in the Northeastern Transvaal. D.Sc. Dissertation (unpubl.). University of Pretoria, Pretoria, pp. 207.
Schwellnus, J.S.I., Engelbrecht, L.N.J., Coertze, F.J., Russel, H.D., Malherbe, S.J., van Rooyen, D.P., Cooke, R., 1962. The Geology of the Olifants River Area, Transvaal. Geological Survey of South Africa, Explanation of Sheets 2429B (Chuniespoort) and 2430A (Wolkberg).
Scoates, J.S., Friedman, R.M., 2008. Precise age of the platiniferous Merensky Reef, Bushveld Complex, South Africa, by the U-Pb zircon chemical abrasion ID-TIMS technique. Econ. Geol. 103, 465–471.
Scoon, R.N., 2002. A new occurrence of Merensky Reef on the flanks of the Zaaikloof Dome, Northeastern Bushveld Complex: relationship between diapirism and magma replenishment. Econ. Geol. 97, 1037–1049.
Scoon, R.N., Mitchell, A., 1994. Discordant iron-rich ultramafic pegmatites in the Bushveld Complex and their relationship to iron-rich intercumulus and residual liquids. J. Petrol. 35, 881–917.
Scoon, R.N., Mitchell, A.A., 2012. The Upper Zone of the Bushveld Complex at Roossenekal, South Africa: Geochemical stratigraphy and evidence of multiple episodes of magma replenishment. S. Afr. J. Geol. 115 (4), 515–534.
Sharpe, M.R., 1985. Strontium isotope evidence for preserved density stratification in the Main Zone of the Bushveld Complex, South Africa. Nature 316, 119–126.
Sharpe, M.R., Chadwick, B., 1982. Structures in Transvaal Sequence rocks within and adjacent to the eastern Bushveld Complex. Transactions of the Geological Society of South. Africa 85, 29–41.
Sharpe, M.R., Snyman, J.A., 1980. A model for the emplacement of the eastern compartment of the Bushveld Complex. Tectonophysics 65, 85–110.
Smith, D.S., Basson, I.J., 2006. Shape and distribution analysis of Merensky Reef potholing, Northam Platinum Mine, western Bushveld Complex: implications for pothole formation and growth. Mineral. Deposita 41, 281–295.
Stannistreet, I.J., McCarthy, T.S., 1991. Changing tectono-sedimentary scenarios relevant to the development of the late Archaean Witwatersrand Basin. J. Afr. Earth Sci. 13, 65–81.
Stannistreet, I.J., McCarthy, T.S., Charlesworth, E.G., Myers, R.E., Armstrong, R.A., 1986. Pre-Transvaal wrench tectonics along the northern margin of the Witwatersrand Basin, South Africa. Tectonophysics 1131, 53–74.
Tchikaya, E.B., Chouteau, M., Keating, P., Shamsipour, P., 2016. 3D unconstrained and geologically constrained stochastic inversion of airborne vertical gravity gradient data. Explor. Geophys. 47 (1), 67–84.
Treloar, M.L., Steenkamp, C.J., 2000. Design guidelines and practical considerations for shallow multiseam chrome Mining at Samancor-Western Chrome Mines. In: Proc. South African National Institute of Rock Engineers Symposium: Keeping it up in the Bushveld and Advances in Support Technology. Rustenburg, South Africa.
Truter, F.C., 1955. Modern concepts of the Bushveld Igneous Complex. C.C.T.A. South Regional Communications in. Geology 1, 77–87.
Tyler, R., Tyler, N., 1996. Stratigraphic and structural controls on gold mineralization in the Pilgrim's Rest goldfield, eastern Transvaal, South Africa. Precambrian Res. 79 (1–2), 141–169.
Uken, R., 1999. The Geology and Structure of the Bushveld Complex Metamorphic Aureole in the Olifants River area. Unpub. PhD. Thesis. University of Natal, South Africa, pp. 277.

Uken, R., Gerya, T.V., Reinhardt, J., Maresch, W., Watkeys, M.K., Clarke, B.M., 2003. Cold fingers in a hot magma: Country-rock diapirs triggered by the Bushveld Layered Intrusion, South Africa. Trans. Am. Geophys. Union 83 (47) (Fall Meeting Abstract T22A-1139).
Uken, R., Watkeys, M.K., 1997a. Diapirism initiated by the Bushveld Complex, South Africa. Geology 25, 723–726.
Uken, R., Watkeys, M.K., 1997b. An interpretation of mafic dyke swarms and their relationship with major mafic magmatic events on the Kaapvaal Craton and Limpopo Belt. S. Afr. J. Geol. 100, 341–348.
Van der Merwe, M., 2007. The occurrence of the Critical Zone along the exposed southeastern sector of the eastern Bushveld Complex. S. Afr. J. Geol. 110, 617–630.
Van der Merwe, M.J., 1976. The layered sequence of the Potgietersrus limb of the Bushveld Complex. Econ. Geol. 71, 1337–1351.
Van der Merwe, M.J., 1978. The Geology of the Basic and Ultramafic Rocks of the Potgietersrus Limb of the Bushveld Complex. Ph.D. thesis. University Witwatersrand, pp. 176.
Van der Merwe, M.J., 1998. Platiniferous horizons of the Potgietersrus limb of the Bushveld Complex. In: 8th International Platinum Symposium. Abstracts. The Geological Society of South Africa and the South African Institute of Mining and Metallurgy, Marshalltownpp. 407–409.
Van der Merwe, M.J., 2008. The geology and structure of the Rustenburg layered suite in the Potgietersrus/Mokopane area of the Bushveld Complex, South Africa. Mineral. Deposita 43, 405–419.
Van Tongeren, J.A., Mathez, E.A., 2009. The geochemical relationship between the Bushveld Complex and Rooiberg felsites and its petrologic and dynamic significance. In: Abstract, American Geophysical Union, Fall Meeting 2009.
Van Tongeren, J.A., Mathez, E.A., Kelemen, P.B., 2010. A Felsic End to Bushveld Differentiation. J. Petrol., vol. 51 (9), 1891–1912.
Vermaak, C.F., 1970. The geology of the lower portion of the Bushveld Complex and its relationship to the floor rocks in the area west of Pilansberg, western Transvaal. Special publication of the Geological Society of South Africa 1, 242–262.
Vermaak, C.F., Hendricks, L.P., 1976. A review of the mineralogy of the Merensky Reef, with specific reference to new data on precious metal mineralogy. Econ. Geol. 71, 1244–1269.
Vermaak, C.F., Von Gruenewaldt, G., 1986. In: Anhaeusser, C.R., Maske, S. (Eds.), Introduction to the Bushveld Complex. Mineral Deposits of Southern Africa. Geological Society of South Africa, pp. 1021–1029.
Verwoerd, W.J., 1963. Die geologise struktuur van die Krokodilrivierfragment. Trans. Geol. Soc. S. Afr. 66, 49–66.
Viljoen, M.J., 1994. A review of regional variations in facies and grade distribution of the Merensky Reef, western Bushveld Complex, with some mining implications. In: Proc. 15th CMMI Congress, South African Institute of Mining and Metallurgypp. 183–194.
Viljoen, M.J., 1999. The nature and origin of the Merensky Reef of the western Bushveld Complex based on geological facies and geophysical data. S. Afr. J. Geol. 102 (3), 221–239.
Viljoen, M.J., Hieber, R., 1986. The Rustenburg section of Rustenburg platinum mines with reference to the Merensky Reef. In: Anhaeusser, C.R., Maske, S. (Eds.), Mineral Deposits of Southern Africa. vol. 1107. Geological Society of South Africa, pp. 34.
Viljoen, M.J., Schurmann, L.W., 1998. In: Wilson, M.G.C., Annhaeusser, C.R. (Eds.), Platinum-group metals. The Mineral Resources of South Africa, 6th edition. Council for Geoscience, pp. 532–568.
Viljoen, M.J., Scoon, N., 1985. The distribution and main geologic features of discordant bodies of iron-rich ultramafic pegmatite in the Bushveld Complex. Econ. Geol. 80, 1109–1128.
Visser, D.J.L., 1957. The structural evolution of the Union. Proceedings of the Geological Society of South Africa 60, 13–49.
Von Gruenewaldt, G., 1979. A review of some recent concepts of the Bushveld Complex with particular reference to the sulphide mineralization. Can. Mineral. 17, 233–256.
Waldeck, H.G., Sturgeon, M., van der Merwe, A.J., 2007. Definitive Feasibility Study on the Ruighoek and Tuschenkomst Properties. SRK Project Number 376482, SRK Consulting, South Africa. pp. 127.
Wallmach, T., Hatton, C.J., Droop, G.T.R., 1989. Extreme facies of contact metamorphism developed in calc-silicate xenoliths in the eastern Bushveld Complex. Can. Mineral. 27, 509–523.
Walraven, F., 1974. Tectonism during emplacement of the Bushveld Complex and the resulting fold structures. Trans. Geol. Soc. S. Afr. 77, 323–328.
Walraven, F., 1981. The Geology of the Rustenburg Area: Explanation of Geological Map Sheet 2526. South Africa Geological Survey. pp. 37.
Walraven, F., 1987. Geochronology and isotope geochemistry of Bushveld Complex rocks from the Fairfield borehole at Moloto, northeast of Pretoria. S. Afr. J. Geol. 351–360.
Walraven, F., 1989. The Geology of the Pilgrims Rest Area. Explanation to Sheet 2430 (Pilgrims Rest). South Africa. pp. 1180.
Walraven, F., 1997. Geochronology of the Rooiberg Group, Transvaal Supergroup, South Africa. Information Circular. vol. 316 Economic Geology Research Unit, University of the Witwatersrand, Johannesburg, South Africa.
Walraven, F., Armstrong, R.A., Kruger, F.J., 1990. A chronostratigraphic framework for the north-central Kaapvaal Craton, the Bushveld Complex and Vredefort structure. Tectonophysics 171, 23–48.
Walraven, F., Darracott, B.W., 1976. Quantitative interpretation of a gravity profile across the western Bushveld Complex. Trans. Geol. Soc. S. Afr. 79, 22–26.
Webb, S.J., Ashwal, L.D., Cawthorn, R.G., 2011. Continuity between eastern and western Bushveld Complex, South Africa, confirmed by xenoliths from kimberlite. Contrib. Mineral. Petrol. 162, 101–107.
Webb, S.J., Cawthorn, R.G., Nguuri, T., James, D., 2004. Gravity modelling of Bushveld Complex connectivity supported by Southern African Seismic Experiment results. S. Afr. J. Geol. 107, 207–218.
Wilcox, R.E., Harding, T.P., Seely, D.R., 1973. Basic wrench tectonics. Am. Assoc. Pet. Geol. Bull. 57, 74–96.
Willemse, J., 1959. The floor of the Bushveld Igneous Complex and its relationships with special reference to the eastern Transvaal. Proceedings of the Geological Society of South. Africa 62, 11–14.
Willemse, J., 1964. A brief Outline of the geology of the Bushveld Complex. In: Haughton, S.H. (Ed.), The Geology of Some Ore Deposits of Southern Africa. Geological Society of South Africa II, pp. 91–128.
Willemse, J., 1969. The geology of the Bushveld Igneous Complex - the largest repository of magmatic ore deposits in the world. Econ. Geol. Monogr. 4, 1–22.
Williams, N., de Wet, B., Kekana, S., Nielsen, S., Broughton, D., 2016. Applying Advanced Gravity and Magnetic Inversion Methods to Expand the Platreef PGE-Ni-Cu Resource in the Bushveld Complex ASEG-PESA-AIG 2016 1 August 21–24, 2016, Adelaide, Australia.
Wilson, A.H., 2012. A Chill Sequence to the Bushveld Complex: Insight into the First Stage of Emplacement and Implications for the Parental Magmas. J. Petrol. 53, 1123–1168.
Wilson, A.H., 2015. The Earliest Stages of Emplacement of the Eastern Bushveld Complex: Development of the Lower Zone, Marginal Zone and Basal Ultramafic Sequence. J. Petrol. 56 (2), 347–388.
Wilson, A.H., Chunnett, G., 2010. In: Jugo, P., Mungall, J., Brown, H. (Eds.), New Insight into the Stratigraphy, Emplacement and Evolution of the Basal Ultramafic Succession in the Eastern Bushveld Complex, South Africa. 11th International Platinum Symposium, June, 2010, Sudbury, Extended abstracts. http://11thIPS.laurentian.ca.
Wilson, J.R., Cawthorn, R.G., Kruger, F.J., Grundvig, S., 1994. A major unconformity in the western Bushveld Complex: the northern “gap”. S. Afr. J. Geol. 97, 462–472.
Worst, B.G., 1959. Discussion of paper by C.A. Cousins (1959). Trans. Geol. Soc. S. Afr. 62, 193.
Zeh, A., Ovtcharova, M., Wilson, A.H., Schaltegger, U., 2015. The Bushveld Complex was emplaced and cooled in less than one million years - results of zirconology, and geotectonic implications. Earth Planet. Sci. Lett. 418, 103–114.